Quantitative Modeling and Analysis of the Transforming Growth Factor β Signaling Pathway

Seung-Wook Chung,[†] Fayth L. Miles,[‡§] Robert A. Sikes,[‡§] Carlton R. Cooper,[‡§] Mary C. Farach-Carson,[‡§] and Babatunde A. Ogunnaike[†§*]

[†]Department of Chemical Engineering, [‡]Department of Biological Sciences, and [§]Center for Translational Cancer Research University of Delaware, Newark, Delaware 19716

ABSTRACT Transforming growth factor β (TGF-β) signaling, which regulates multiple cellular processes including proliferation, apoptosis, and differentiation, plays an important but incompletely understood role in normal and cancerous tissues. For instance, although TGF-β functions as a tumor suppressor in the premalignant stages of tumorigenesis, paradoxically, it also seems to act as a tumor promoter in advanced cancer leading to metastasis. The mechanisms by which TGF-β elicits such diverse responses during cancer progression are still not entirely clear. As a first step toward understanding TGF-β signaling quantitatively, we have developed a comprehensive, dynamic model of the canonical TGF-β pathway via Smad transcription factors. By describing how an extracellular signal of the TGF-β ligand is sensed by receptors and transmitted into the nucleus through intracellular Smad proteins, the model provides quantitative insight into how TGF-β-induced responses are modulated and regulated. Subsequent model analysis shows that mechanisms associated with Smad activation by ligand-activated receptor, nuclear complex formation among Smad proteins, and inactivation of ligand-activated Smad (e.g., degradation, dephosphorylation) may be critical for regulating TGF-β-targeted functional responses. The model was also used to predict dynamic characteristics of the Smad-mediated pathway in abnormal cells, from which we generated four testable hypotheses regarding potential mechanisms by which TGF-β's tumor-suppressive roles may appear to morph into tumor-promotion during cancer progression.

INTRODUCTION

Transforming growth factor-β (TGF-β) proteins are members of a superfamily of secreted cytokines that control a diverse array of cellular processes including cell proliferation, differentiation, motility, adhesion, angiogenesis, apoptosis, and immune surveillance (1–3). The TGF-β signaling cascade begins when activated TGF-β binds to and brings together Type I and Type II TGF-β receptor serine/threonine kinases on the cell surface, whereby the Type II receptor phosphorylates and activates the Type I receptor. The activated Type I receptor, in turn, propagates the signal through phosphorylation of receptor-bound (R-)Smad transcription factors (Smad2/3 and Smad1/5/8) at the carboxy-terminal SXS motif. The activated R-Smads form hetero-oligomers with a common partner or co-Smad, namely Smad4, and rapidly translocate into the nucleus where they undergo continuous nucleocytoplasmic shuttling by interacting with the nuclear pore complex. Once in the nucleus, activated Smad complexes bind to specific promoters and ultimately regulate expression of target genes through interactions with other transcriptional co-activators and co-repressors, generating ~500 gene responses in a cell- and context-specific manner (1,3–6).

The TGF-β signaling pathway has become an attractive but difficult target for oncology drug development because of its apparently paradoxical roles in tumorigenesis and metastasis. In normal and early phase tumorigenic epithelial cells, TGF-β functions as a potent tumor suppressor primarily by inducing cell cycle arrest and apoptosis. However, in the intermediate and late stages of carcinogenesis, tumor cells become resistant to the growth inhibitory effects of TGF-β and show elevated expression of TGF-β. The ligand is overexpressed in clinical cancer samples, with increasing levels correlating with poor clinical outcomes (7–9). The role of TGF-β therefore seems to become one of tumor promotion, apparently supporting growth, subverting the immune system, and also facilitating angiogenesis, epithelial to mesenchymal transition (EMT), and invasion. This finding has created the widely held perception that TGF-β acts as a tumor promoter in advanced tumorigenesis and metastasis (10–12). Although it is known that most cancer cell lines representing the entire spectrum of tumor progression have active TGF-β signaling pathways, detailed mechanisms of how a single stimulus, TGF-β, induces such a diverse array of responses during cancer progression remains poorly understood.

One of the major obstacles to understanding TGF-β biology is the complexity of the signaling cascade system in which a variety of signaling components that change dynamically over different time scales interact with one another. Quantitative understanding and analysis of such a complex regulatory circuit are not possible via qualitative human intuition alone; mathematical descriptions that lead to predictive models are necessary, and have become useful in improving our understanding of this complex signaling

Submitted June 18, 2008, and accepted for publication November 12, 2008.

*Correspondence: ogunnaike@UDel.Edu

Editor: Arthur Sherman.

0006-3495/09/03/1733/18 $2.00

doi: 10.1016/j.bpj.2008.11.050

pathway. Whereas significant progress has been made in understanding the biochemistry of the TGF-β pathway, quantitative modeling of the TGF-β signaling system remains in its infancy; several models have been published, but each has focused on restricted portions of the pathway. Vilar et al. (13) explored a model of TGF-β signal processing at the receptor level. They modeled TGF-β receptor trafficking events taking place concurrently at the plasma membrane and in endosomes. They incorporated the processes of receptor internalization into endosomes, recycling to the plasma membrane, constitutive and ligand-induced receptor degradation, and receptor protein synthesis in their model. In contrast, Clarke et al. (14) focused on intracellular signaling via the Smad-mediated pathway where they incorporated several steps into both the cytoplasmic and the nuclear events such as R-Smad phosphorylation and dephosphorylation, and nucleocytoplasmic shuttling of Smad proteins. However, this model does not show a direct relationship between an extracellular TGF-β ligand and intracellular responses because signaling is initiated by the activated receptor complex, not by TGF-β ligand itself. The dynamic behavior of the ligand-stimulated receptor complex was described by a simple decreasing exponential function.

Melke and coworkers (15) presented a minimalist model of TGF-β signal transduction in endothelial cells for which downstream signaling is effected via two Type I receptors (ALK1 for Smad1/5/8 and ALK5 for Smad2/3). This model used significantly simplified signaling mechanisms in the pathway at both the surface and the intracellular levels, and incorporated an inhibitory protein, Smad7, to implement a simplistic feedback loop. A more recent contribution from Zi and Klipp (16) offered more detailed receptor trafficking than the Vilar model, and incorporated a simplified Smad-pathway and ligand-induced receptor inhibition. The latest model by Schmierer et al. (17) focused on Smad nucleocytoplasmic dynamics, providing a better description of the Smad pathway than the earlier models; but this model still lacks a detailed description of the dynamic process of receptor trafficking and TGF-β-induced receptor activation.

Thus, although these previous modeling efforts have provided adequate descriptions of various aspects of the TGF-β signaling pathway, none provides a sufficiently comprehensive and/or realistic description of the signaling cascades, limiting their ability to facilitate understanding and analysis of the complex TGF-β system and to predict system behavior under aberrant conditions accurately. In particular, the oversimplification or omission of some important steps in the pathway used in these models limits their suitability for use in attempting to unravel the mystery of the seemingly contradictory roles of TGF-β in cancer progression. Such applications require a more comprehensive and more realistic description of the signaling pathway.

As a first step in understanding TGF-β signaling quantitatively, we present in this study, an integrated TGF-β pathway model in epithelial cells, by incorporating transduction of an extracellular signal (i.e., the ligand-binding, receptor activation and trafficking), transmission of the signal (i.e., the canonical downstream Smad pathway), and by modifying and adding some important mechanisms (sequential receptor activation, protein synthesis, constitutive and ligand-induced degradation of signaling components, nuclear dephosphorylation of Smad, nuclear Smad complex formation, etc.), in accordance with the most up-to-date information available about the TGF-β signaling system. The result, as described below, is a system of ordinary differential equations (ODEs) from which, given as input the concentration of the extracellular TGF-β ligand, one obtains as the primary output of interest, namely the dynamic behavior of the activated Smad2-Smad4 complex in the nucleus, which ultimately determines target gene expression and cellular responses, along with the dynamics of other intermediate signaling component proteins. Through simulation and model analysis, our model provides insight into the signal-response relationship between the binding of TGF-β to its receptor at the cell surface and the activation of downstream effectors in the signaling cascade. In particular, we use the model to carry out ''in silico mutations'' from which we generate several hypotheses regarding potential mechanisms for how TGF-βs tumor-suppressive roles may seem to morph into tumor-promoting roles.

MATERIALS AND METHODS

Model development

The following is a description of the essential molecular processes on which the model is based.

The binding of ligand to signaling receptors

TGF-β ligands activate signaling by binding to and bringing together pairs of Type I and Type II receptors. Specifically, the active form of dimeric TGF-β (assumed to be a single unit) binds to the ectodomain of dimeric Type II receptor (TβRII, designated as RII in the kinetic scheme) and forms a catalytically active TGF-β-RII complex (designated as TGFβ-RII). The activated TGFβ-RII complex subsequently interacts with Type I receptor (TβRI or ALK5, designated as RI), and activates it, forming a TGFβ-RII-RI complex (designated as R^C) at the cell surface (1), which is ready for downstream signaling.

Receptor internalization and recycling

It has been reported that TGF-β receptors are continuously internalized via clathrin-coated pits into early endosomes and are recycled to the plasma membrane for signaling, even in the absence of ligand (18,19). Vilar et al. (13) have modeled the dynamic behavior of TGF-β receptors, considering receptor internalization and recycling. We adopt the approach of Vilar and coworkers, using first-order kinetics to describe receptor trafficking.

Smad phosphorylation

Although the receptors for TGF-β signal through both Smad2 and Smad3 proteins in epithelial cells, we select Smad2 to represent the R-Smads, because the two are virtually identical kinetically; furthermore, Smad2 is ~12-fold more abundant than Smad3 (14,20). Based on previous studies showing that Smad activation for signaling requires internalization of the

TGF-β receptor (18,21,22), we assume that Smad2 in the cytoplasm interacts first with the activated ligand-receptor complexes internalized into early endosomes, and then is phosphorylated.

Smad heteromerization

The stoichiometry of active R-Smad/Smad4 heteromeric complexes remains a controversial topic; the R-Smad/Smad4 complexes have been suggested to function as either dimers or trimers after homodimerization of R-Smad (23–28). For simplicity, we assume that phosphorylated Smad2 and Smad4 form a heterodimeric complex. In principle, receptor-activated R-Smads, after undergoing a conformational change to allow for association with other activated Smads, could associate with either another R-Smad and/or Smad4 in the cytoplasm first, followed by their entry into the nucleus as RSmad-Smad4 complexes; alternatively, these complexes could form after R-Smads translocate into the nucleus (29,30). The latter implies nuclear import of monomeric or dimeric phosphorylated R-Smads, which is discussed next.

Nucleocytoplasmic shuttling

In the basal state, both R-Smads and Smad4 are predominantly localized in the cytoplasm. However, on ligand stimulation, both species rapidly accumulate in the nucleus (30,31). It is becoming clear that these distributions are not static; rather both R-Smads and Smad4 shuttle continuously between the cytoplasm and nucleus regardless of TGF-β stimulation, ultimately reaching a dynamic equilibrium (20,32–34). We therefore consider both import and export steps for monomeric R-Smad and Smad4 in our model. Although it is widely believed that activated R-Smads translocate into the nucleus in the heteromeric complex form with Smad4, it has been observed that complex formation of TGF-β-induced R-Smads with Smad4 is not always necessary for their accumulation in the nucleus (30,35,36). We therefore include nuclear import of receptor-phosphorylated R-Smad monomers in the cytoplasm in the model.

It has been suggested that the nuclear export signal of Smad4 may be masked through complex formation with activated R-Smads (3,20,30), resulting in nuclear accumulation of Smad4 after TGF-β stimulation. Also, a recent study proposed that only monomeric unphosphorylated Smad2 is capable of export so that the phosphorylated complex form of Smad2 is trapped in the nucleus (32). These observations provide the basis for our assumption that translocation of activated monomeric R-Smads and heteromeric RSmad-Smad4 complex is unidirectional.

Developing realistic mathematical descriptions of nucleocytoplasmic shuttling of Smads has been complicated by the complexity of, and uncertainty associated with, the import and export mechanisms that depend on the type of R-Smads. For example, regarding nuclear import, it has been proposed that Smad2, Smad3, and Smad4 enter the nucleus by direct interactions with the nuclear pore complex (37,38). However, it also has been suggested that the nuclear import of Smad3 and Smad4 depends on the nuclear import factor, importin-β (39,40). On the other hand, Smad4 export from the nucleus is mediated by CRM-1 (chromosomal region maintenance-1) nuclear export factor, whereas R-Smad export is independent of CRM-1 and simply may be mediated by direct interactions with nucleoporins (37,38). In the absence of a consensus, we opt for a simple mechanism of nucleocytoplasmic shuttling, assuming first-order kinetics for both import and export steps.

Dissociation and dephosphorylation

Suspecting the existence of unidentified R-Smad phosphatases, it has been proposed that R-Smads should undergo cycles of phosphorylation and dephosphorylation to shuttle between the cytoplasm and the nucleus in the presence of a TGF-β signal (20,30,32,34). Lin et al. (41) confirmed this postulate about the existence of the phosphatases by identifying a Smad-specific phosphatase, PPM1A, that directly dephosphorylates Smad2 and Smad3 to limit their activation. Thus, it is believed that dephosphorylation of Smad2 by PPM1A or other phosphatase leads to dissociation of R-Smad-Smad4 complexes to terminate the TGF-β signaling on receptor deactivation, or to recycle R-Smads in the presence of a prolonged TGF-β signal, implying that dephosphorylation precedes dissociation. However, because a receptor-phosphorylated R-Smad monomer also may form a complex with Smad4 after R-Smads translocate into the nucleus as well as in the cytoplasm, we cannot rule out the possibility of activated Smad complex dissociation before dephosphorylation (42). We therefore include both steps in our model. It has been reported that PPM1A is primarily localized in the nucleus regardless of TGF-β stimulation (41), which supports the previous suggestions that R-Smad dephosphorylation seems to occur in the nucleus (29,34). This leads us to take only nuclear dephosphorylation into account in our model.

Protein degradation

Each signaling component in the pathway is irreversibly eliminated via different mechanisms. First, degradation of receptors can occur via two different modes: ligand-dependent degradation targeted by Smad7-Smurf2 via the lipid-raft caveolar pathway, and ligand-independent (or constitutive) degradation (13,19). We assume that ligand-unbound Type I and Type II receptors, and ligand-induced receptor complexes at the surface are terminated in the pathway, as suggested by Vilar et al. (13). Second, it has been reported that receptor-activated Smad2 undergoes TGF-β-induced, ubiquitin-dependent degradation (43). It also has been suggested that proteasomal degradation of Smad2 is likely to occur in the nucleus, mediated by the interaction of Smurf2 with phosphorylated Smad2 (44), whereas Smurf2 is known as a cytoplasmic protein (45). Thus, it remains unclear whether Smad2 is targeted to either nuclear or cytoplasmic proteasomes or both. In this study, we assume that monomeric receptor-phosphorylated Smad2 is irreversibly removed by nuclear proteasomes, and un- and/or dephosphorylated single Smad2 is eliminated in the cytoplasm. Last, it has been reported that ubiquitination and proteasomal degradation of Smad4 is mediated by its direct interaction with Jab1, known as a coactivator of c-Jun and subunit of COP9 signalosome (46). We assume that Smad4 is eliminated in the cytoplasm.

Protein synthesis

Describing the production of proteins in a mathematical manner is quite complicated because of the uncertainty and complexity of the nuclear mechanisms for gene expression. Alternatively, many mathematical models of cell signaling that deal with proteins alone assume constant production of the signaling components (13,15,47). Likewise we also assume that the 4 major signaling components (i.e., Type I and Type II receptors, Smad2, and Smad4) are produced under stationary conditions regardless of the presence of ligand.

The components of the overall TGF-β signaling pathway as featured in our model are depicted in Fig. 1. The resulting model is a system of 17 nonlinear ODEs with 37 kinetic parameters arising from chemical reactions represented by mass action kinetics. The complete set of model equations, shown in Table 1, is integrated using the ODE15s routine of MATLAB 7.1 (The MathWorks, Natick, MA).

Our model is based on three well-mixed compartments with the basic cellular characteristics defined for human keratinocyte HaCaT cells as follows: the extracellular (calculated as 1 mL/10^6 cells), the cytoplasmic, and the nuclear compartments. The cell is idealized as a sphere with a diameter of 15 μm, resulting in a cell volume of 1.5×10^{-12} L. Because, according to Schmierer and Hill (32), an average cytoplasmic/nuclear volume ratio for HaCaT cells is ~3, we choose the values 1.13×10^{-12} L and 3.75×10^{-13} L, respectively, for the volumes of the cytoplasmic and nuclear compartments.

Initial conditions

We select the value 10,000 for the total number of TGF-β receptor molecules in the basal state. (This number is the median of the values presented in the literature (48)). Assuming that Type I and Type II receptors are distributed

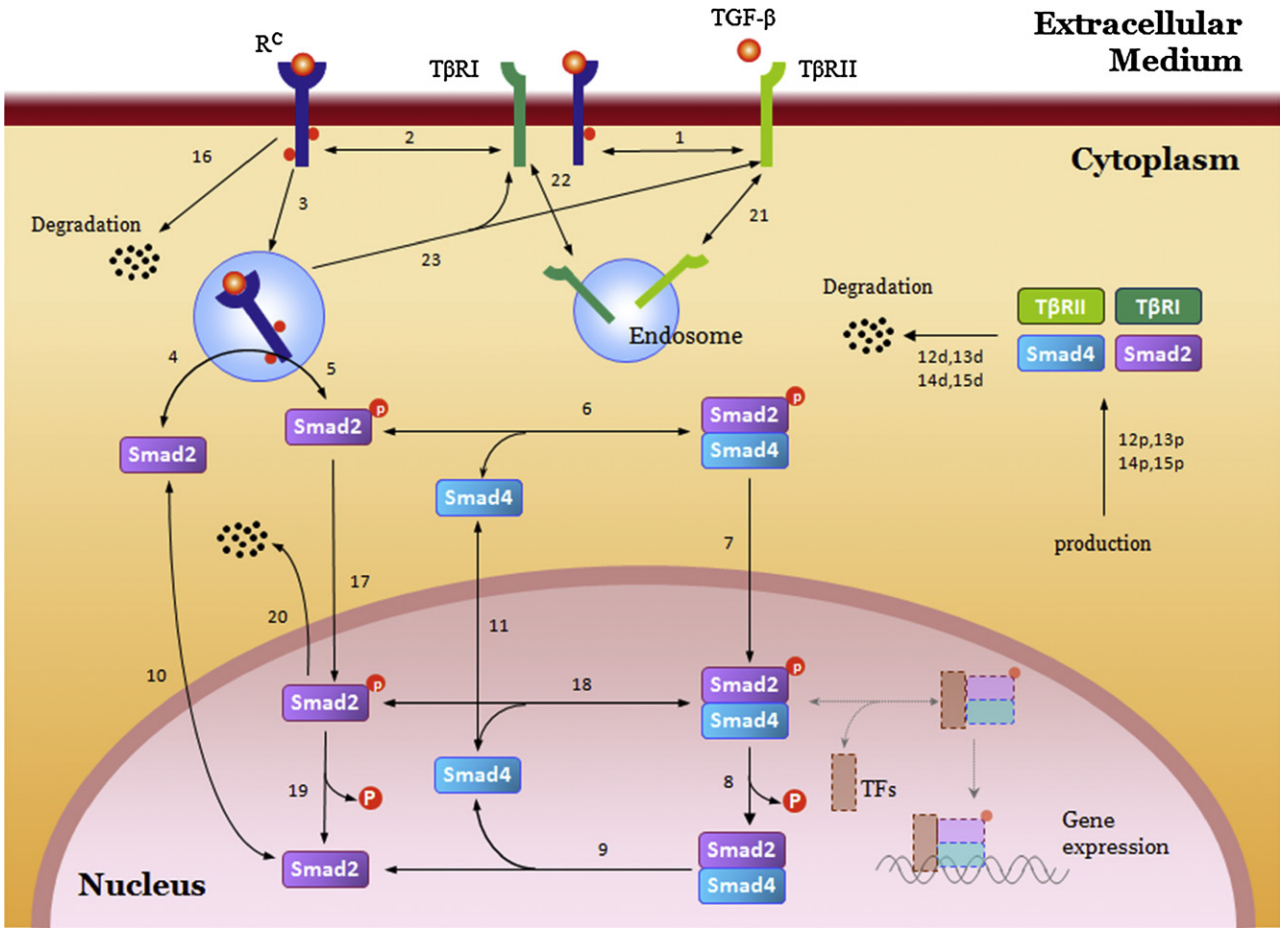

FIGURE 1 Schematic representation of the pathway components in the integrated model. Numbers in the cartoon refer to the chemical reaction indices in Table 1.

evenly, we choose the value 5,000 each for the initial number of Type I and Type II receptor molecules. From recent observations that receptors are internalized continuously and recycled to the surface whether ligand is present or not, we assume that only 10% of total receptors are present in the plasma membrane at any one time and that the remaining 90% of total receptors are sequestered in endosomes (13,18,19). We also selected 100,000 to represent the total number of each Smad effector, in our case, Smad2 and Smad4 molecules (14). In the basal state, 15% of total Smad2

TABLE 1 Model equations

$$v_1 = k_{1a}[TGF\beta][RII] - k_{1d}[TGF\beta : RII]$$
$$v_2 = k_{2a}[TGF\beta : RII][RI] - k_{2d}[R^C]$$
$$v_3 = k_{3int}[R^C]$$
$$v_4 = k_{4a}[R^C_{in}][S2_{cyt}] - k_{4d}[R^C_{in} : S2_{cyt}]$$
$$v_5 = k_{5cat}[R^C_{in} : S2_{cyt}]$$
$$v_6 = k_{6a}[pS2_{cyt}][S4_{cyt}] - k_{6d}[pS2S4_{cyt}]$$
$$v_7 = k_{7imp}[pS2S4_{cyt}]$$
$$v_8 = k_{8dp}[pS2S4_{nuc}]$$
$$v_9 = k_{9d}[S2S4_{nuc}]$$
$$v_{10} = k_{10imp}[S2_{cyt}] - k_{10exp}[S2_{nuc}]$$
$$v_{11} = k_{11imp}[S4_{cyt}] - k_{11exp}[S4_{nuc}]$$
$$v_{12} = k_{12syn} - k_{12deg}[RII]$$
$$v_{13} = k_{13syn} - k_{13deg}[RI]$$
$$v_{14} = k_{14syn} - k_{14deg}[S2_{cyt}]$$
$$v_{15} = k_{15syn} - k_{15deg}[S4_{cyt}]$$
$$v_{16} = (k_{16deg} + k_{16lid})[R^C]$$
$$v_{17} = k_{17imp}[pS2_{cyt}]$$
$$v_{18} = k_{18a}[pS2_{nuc}][S4_{nuc}] - k_{18d}[pS2S4_{nuc}]$$
$$v_{19} = k_{19dp}[pS2_{nuc}]$$
$$v_{20} = k_{20lid}[pS2_{nuc}]$$
$$v_{21} = k_{21int}[RII] - k_{21rec}[RII_{in}]$$
$$v_{22} = k_{22int}[RI] - k_{22rec}[RI_{in}]$$
$$v_{23} = k_{23rec}[R^C_{in}]$$

$$\frac{d[RII]}{dt} = -v_1 + v_{12} - v_{21} + v_{23}$$
$$\frac{d[TGF\beta:RII]}{dt} = v_1 - v_2$$
$$\frac{d[RI]}{dt} = -v_2 + v_{13} - v_{22} + v_{23}$$
$$\frac{d[R^C]}{dt} = v_2 - v_3 - v_{16}$$
$$\frac{d[R^C_{in}]}{dt} = v_3 - v_4 + v_5 - v_{23}$$
$$\frac{d[R^C_{in}:S2_{cyt}]}{dt} = v_4 - v_5$$
$$\frac{d[S2_{cyt}]}{dt} = -v_4 - v_{10} + v_{14}$$
$$\frac{d[pS2_{cyt}]}{dt} = v_5 - v_6 - v_{17}$$
$$\frac{d[pS2S4_{cyt}]}{dt} = v_6 - v_7$$
$$\frac{d[pS2S4_{nuc}]}{dt} = v_7 - v_8 + v_{18}$$
$$\frac{d[S2S4_{nuc}]}{dt} = v_8 - v_9$$
$$\frac{d[S2_{nuc}]}{dt} = v_9 + v_{10} + v_{19}$$
$$\frac{d[S4_{nuc}]}{dt} = v_9 + v_{11} - v_{18}$$
$$\frac{d[S4_{cyt}]}{dt} = -v_6 - v_{11} + v_{15}$$
$$\frac{d[pS2_{nuc}]}{dt} = v_{17} - v_{18} - v_{19} - v_{20}$$
$$\frac{d[RII_{in}]}{dt} = v_{21}$$
$$\frac{d[RI_{in}]}{dt} = v_{22}$$

and 13% of total Smad4 are assumed to reside in the nucleus (32). All other species are set to zero initially.

Model parameter estimation

To carry out simulations with the model requires specific values for the reaction kinetic parameters. Parameter estimation, the procedure for determining from a set of experimental data the values of unknown model parameters, continues to receive attention in systems biology. However, currently there is no consensus as to how to deal with such important related issues as parameter identifiability, the possibility of multiple local minima, and high computational costs. The approach taken in this study is summarized below.

Initial rough estimation

Several kinetic parameter values were determined through an extensive literature search; some were computed using available in vitro experimental data; we also used physical constraints to determine others. For instance, the dissociation constant $K_d = k^{off}/k^{on}$ is available for protein-protein binding reactions, whereas the separate on- and off-rates, k^{on} and k^{off}, are not. Under these conditions, we chose an initial estimate for k^{on} by comparison with similar steps in other kinase pathways and computed the corresponding k^{off} as $k^{off} = K_d \times k^{on}$. The remaining unknown parameters were provided with initial estimates and reasonable upper and lower bounds by comparison with similar circumstances in the literature (e.g., similar steps in previous models or other signaling pathway models) and from known physical limitations (e.g., the diffusion-limited rates, 10^8–10^9 M^{-1} s^{-1} (49)).

Parametric sensitivity analysis

To identify which parameters are the most important and which must therefore be estimated most precisely, using the set of initial estimates determined in Step 1 above, we carried out local parameter sensitivity analysis to determine the effect of parametric changes on the set of five system responses of interest for which experimental measurements are available (i.e., total Smad2 in the nucleus and the cytoplasm (30), total phosphorylated Smad2 in the nucleus and the cytoplasm (20,30), and total Smad4 in the nucleus (30)). The computations are based on the following expression for the normalized sensitivity coefficient:

$$NSC_{ij}(t) = \frac{p_j}{y_i}\frac{\partial y_i(t,\mathbf{p})}{\partial p_j}\bigg|_p,\ i = 1,2,\ldots,5; j = 1,\ldots,37,$$

where y and $\mathbf{p}$ respectively denote the system response variables and kinetic parameters. A total of 13 parameters were selected to be estimated more precisely because of their high sensitivity coefficients and/or because we had little or no confidence in their initial values.

Least squares fitting to data

We fit our model predictions simultaneously to corresponding in vitro experimental data from the literature, via local minimization of the sum of squared residual errors:

$$\min_i R(p) = \frac{1}{2}\sum\left(y_i(t,\mathbf{p}) - y_i^*(t)\right)^2,$$

where $y_i(t,\mathbf{p})$ and $y_i^*(t)$ denote, respectively, model predictions for a given trial of parameter values, $\mathbf{p}$, and the corresponding experimental measurements, for each measured variable, i. The experimental data used for the curve-fitting are time courses of i), total Smad2 in the nucleus (30); ii), total Smad2 in the cytoplasm (30); iii), total phosphorylated Smad2 in the nucleus (20); iv), total phosphorylated Smad2 in the cytoplasm (30); and v), total Smad4 in the nucleus (30). We quantified the immunoblot literature data with the Image Processing Toolbox in MATLAB 7.1, and normalized both the experimental data and the corresponding model estimates to the largest intensity point of each data set. The optimum parameter values (constrained to lie within the specified upper and lower bounds) were determined using the nonlinear least square "lsqnonlin" routine of MATLAB 7.1.

Identifiability

We carried out a "practical identifiability" analysis to determine whether the unknown parameters of the postulated model can be estimated uniquely from the available data, following Birtwistle et al. (50). Briefly, approximate local confidence intervals (CI) for the parameter set are given by,

$$CI_i = t_{\alpha/2}^{N_t-N_p}\sqrt{\frac{S}{N_t-N_p}}\sqrt{(\mathbf{Z}^T\mathbf{Z})_{ii}^{-1}},$$

where N_t and N_p respectively denote the number of experimental data time points and the number of parameters to be estimated; $t_{\alpha/2}^{N_t-N_p}$ is the Student's t-distribution statistic evaluated with $N_t - N_p$ degrees of freedom, at confidence level $100(1-\alpha)\%$, (with α as the "tail area probability" typically set at 0.05 to yield a 95% confidence level); S is the sum of squared errors, and $\mathbf{Z}$ is the model sensitivity matrix evaluated at the current parameter values. The i^{th} parameter is said to be practically locally identifiable only if the magnitude of its approximate CI is less than a specified tolerance i.e., $|CI_i| < \varepsilon_i$. We chose tolerances such that the approximate CIs on identifiable parameters were set generously at $\pm$~40%.

Identifiable parameter estimate refinement

Estimated values for identifiable parameters were refined further by repeating Step 4 (local identifiability test) followed by Step 3 (local least squares estimation). After obtaining the "best" estimates of this subset of parameters, we carried out a final least squares estimation of the entire parameter set.

The results of this procedure (final estimates as well as the identifiability status of each parameter) are listed in Table 2.

RESULTS AND DISCUSSION

Model development and validation

Model fit to literature data

A comparison of the model fit to the five sets of in vitro experimental data used for parameter estimation is shown in Fig. 2 *A–E*. First, Fig. 2 *A* shows the model fit to data on total nuclear pSmad2 reported by Inman et al. (20) in response to a step input of 2 ng/ml of TGF-β. Note the good agreement between the model prediction and the data. Furthermore, this dynamic profile also agrees well with other reported experimental results that show the level of nuclear pSmad2 peaking ~45–60 min after TGF-β treatment and declining thereafter, but not to zero, even after 6–8 h (30,51). The model fit to total cytoplasmic pSmad2 data under conditions where protein synthesis is strongly inhibited in the cells, as reported in Pierreux et al. (30), is shown in Fig. 2 *B*. The model shows that the level of cytoplasmic pSmad2 drops sharply after peaking rapidly, and remains very low thereafter. Considering that receptor-activated Smad2 resides either in the cytoplasmic or in the nuclear compartment, it appears as if more of pSmad2 accumulates in the nucleus during active signaling of TGF-β (20,32–34) than elsewhere.

Next, Fig. 2, *C* and *D*, show the model fit to experimental profiles of total Smad2 in the nucleus and the cytoplasm, respectively, under the conditions where cells were treated continuously with 2 ng/mL of TGF-β and 20 μg of the

TABLE 2 Model parameters

Parameter	Reaction step	Value	Unit	Identifiability	Reference
k_{1a}	Ligand binding	6.60 E − 03	$mol^{-1} \cdot min^{-1}$	Unidentifiable	Estimation
k_{1d}	Dissociation	2.98 E − 01	min^{-1}	N/a	(66)
k_{2a}	Association (RI-RII*)	6.60 E − 03	$mol^{-1} \cdot min^{-1}$	Unidentifiable	Estimation
k_{2d}	Dissociation	2.98 E − 01	min^{-1}	N/a	(67)
k_{3int}	Internalization (R^c)	3.95 E − 01	min^{-1}	Unidentifiable	Estimation (13),
k_{4a}	Association (R^c-S2)	1.50 E − 04	$mol^{-1} \cdot min^{-1}$	Unidentifiable	Estimation
k_{4d}	Dissociation	9.71 E − 01	min^{-1}	Unidentifiable	Estimation
k_{5cat}	Turnover (pS2)	4.48 E + 04	min^{-1}	N/A	(68)
k_{6a}	Association (pS2-S4)	6.00 E − 03	$mol^{-1} \cdot min^{-1}$	Unidentifiable	Estimation
k_{6d}	Dissociation	1.46 E + 03	min^{-1}	N/A	(23)
k_{7imp}	Nuclear import (pS2S4)	8.10 E − 01	min^{-1}	Unidentifiable	Estimation
k_{8dp}	Dephosphorylation (pS2S4)	2.52 E − 02	min^{-1}	N/A	Calculation (41)
k_{9d}	Dissociation (S2-S4)	1.01 E − 01	min^{-1}	Unidentifiable	Estimation
k_{10imp}	Nuclear import (S2)	1.62 E − 01	min^{-1}	N/A	(32)
k_{10exp}	Nuclear export (S2)	3.48 E − 01	min^{-1}	N/A	(32)
k_{11imp}	Nuclear import (S4)	2.01 E − 02	min^{-1}	Unidentifiable	Estimation
k_{11exp}	Nuclear export (S4)	1.74 E − 01	min^{-1}	N/A	(32)
k_{12syn}	Protein synthesis (RII)	8.00 E + 00	$mol \cdot min^{-1} \cdot cell^{-1}$	N/A	Calculation
k_{12deg}	Degradation (RII)	2.80 E − 02	min^{-1}	N/A	(13)
k_{13syn}	Protein synthesis (RI)	8.00 E + 00	$mol \cdot min^{-1} \cdot cell^{-1}$	N/A	Calculation
k_{13deg}	Degradation (RI)	2.80 E − 02	min^{-1}	N/A	(13)
k_{14syn}	Protein synthesis (S2)	2.74 E + 01	$mol \cdot min^{-1} \cdot cell^{-1}$	N/A	Calculation
k_{14deg}	Degradation (S2)	6.46 E − 04	min^{-1}	N/A	Calculation (43)
k_{15syn}	Protein synthesis (S4)	5.00 E + 01	$mol \cdot min^{-1} \cdot cell^{-1}$	N/A	Calculation
k_{15deg}	Degradation (S4)	1.20 E − 03	min^{-1}	N/A	Calculation (46)
k_{16deg}	Constitutive deg (R^c)	2.80 E − 02	min^{-1}	N/A	(13)
k_{16lid}	Ligand-induced deg (R^c)	3.95 E − 01	min^{-1}	N/A	(13)
k_{17imp}	Nuclear import (pS2)	5.03 E − 01	min^{-1}	Identifiable	Estimation
k_{18a}	Association (pS2-S4)	1.67 E − 04	$mol^{-1} \cdot min^{-1}$	Unidentifiable	Estimation
k_{18d}	Dissociation	9.09 E − 01	min^{-1}	Unidentifiable	Estimation
k_{19dp}	Dephosphorylation (pS2)	2.52 E − 02	min^{-1}	N/A	As k_{8dp}
k_{20lid}	Ligand-induced deg (pS2)	5.40 E − 03	min^{-1}	Identifiable	Estimation (41)
k_{21int}	Internalization (RII)	3.95 E − 01	min^{-1}	N/A	As k_{3int}
k_{21rec}	Recycling (RII)	3.95 E − 02	min^{-1}	N/A	Calculation (13)
k_{22int}	Internalization (RI)	3.95 E − 01	min^{-1}	N/A	As k_{3int}
k_{22rec}	Recycling (RI)	3.95 E − 02	min^{-1}	N/A	As k_{21rec}
k_{23rec}	Recycling (R^c)	3.95 E − 02	min^{-1}	N/A	As k_{3int}

RI, Type I receptor; RII, Type II receptor; RII*, phosphorylated Type II receptor; R^c, receptor complex; S2, Smad2; S4, Smad4; pS2, phosphorylated Smad2; pS2S4, phosphorylated Smad2-Smad4 complex.

protein synthesis inhibitor, cycloheximide (30). The concentration of TGF-β represents a saturating concentration of this factor expected to maximize signaling parameters. Note how the dynamic pattern of the nuclear Smad2 response appears to be the opposite of the cytoplasmic response. In other words, although the level of nuclear Smad2 reaches a peak and decreases thereafter, the amount of cytoplasmic Smad2 drops correspondingly and then increases. These opposite dynamics may be caused by the shuttling of Smad2 between the cytoplasm and the nucleus via a mechanism that involves the steps of nuclear import and export of Smads; association between nuclear pSmad2 and Smad4; dissociation of the complex; and dephosphorylation of the activated Smad2, and (re)phosphorylation of Smad2 by active receptors.

Finally, Fig. 2 *E* shows the model fit to experimental data from Pierreux et al. (30) for total nuclear Smad4 in response to a step of 2 ng/mL of TGF-β. Although Smad4 shuttles continuously between the cytoplasm and the nucleus in the absence of ligand, TGF-β stimulation allows Smad4 to reside more in the nucleus than in the cytoplasm through complex formation with pSmad2. However, nuclear events such as dephosphorylation of pSmad and dissociation of Smad complex allow nuclear Smad4 to return to the cytoplasm. Thus, nuclear Smad4 reaches peak activity at ~0.5–2 h after ligand addition and declines thereafter (30).

Keeping in mind that the model was fit to these five data sets simultaneously, the resulting agreement between model prediction and data is quite good overall. The inevitable discrepancies between model prediction and experimental data are attributable to the following factors. First, the data sets are from different laboratories and were therefore acquired under nonidentical conditions (e.g., cell culture conditions, cell population, batches of TGF-β, etc.). Thus, model parameters that may be appropriate for one set of experimental data may not be entirely appropriate for another. The optimum model parameters will therefore result from compromises whereby an otherwise ''better'' fit to a single data set is traded off for a reasonable fit to the complete

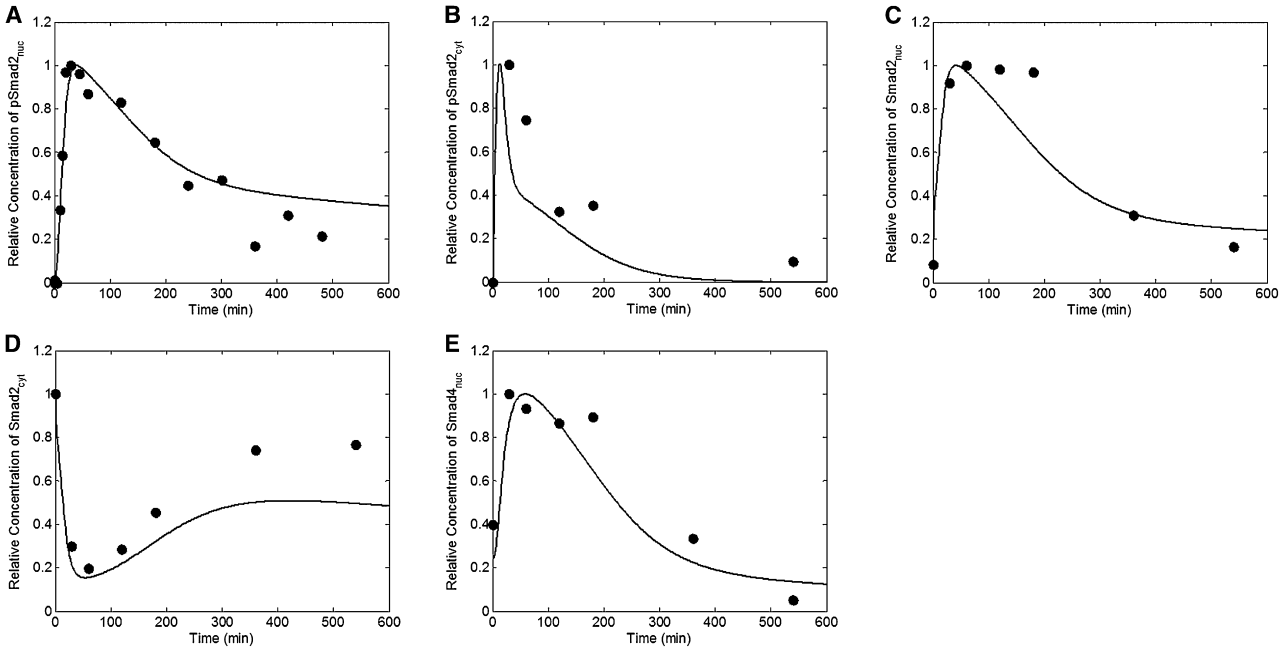

FIGURE 2 Model fit to experimental data: (*A*) total phosphorylated Smad2 in the nucleus (20), (*B*) total phosphorylated Smad2 in the cytoplasm (30), (*C*) total nuclear Smad2 (30), (*D*) total cytoplasmic Smad2 (30), and (*E*) total nuclear Smad4 (30) in response to TGF-β stimulation. Note: to simulate the effects of cycloheximide in (*B–E*), all rates of protein synthesis (k_{12syn}, k_{13syn}, k_{14syn}, and k_{15syn}) were set to zero.

collection. Next, values for kinetic parameters (e.g., dissociation constants, Michaelis constants, etc.) determined from in vitro measurements reported in the literature and used in the model may not exactly correspond to values that obtain under in vivo experimental conditions. Finally, to a lesser extent, the model nonlinearity and constraints raise the distinct possibility that the resulting optimum parameter set may have been found in a local minimum. It is possible to address this problem by using such global optimization methods as genetic algorithm and simulated annealing, but we do not believe that locating parameter estimates in local minima is a sufficiently serious possibility for this specific model to warrant the use of these techniques. Taking all of these considerations into account, the model does a reasonable job of capturing the dynamic behavior of TGF-β signaling as reported in the experimental literature.

Model validation

Because the data sets shown in Fig. 2 *A–E* were used to determine unknown model parameters by minimizing the sum of squared differences between model prediction and data, it is important, before proceeding to use the model, to validate its prediction against a different set of independent experimental data, without adjusting any model parameters. To validate our model in this manner, we compared its predictions to four independent experimental data sets obtained from the literature: i), total phosphorylated Smad2 in the cell (43); ii), ratio of cellular pSmad2 to total Smad2 in response a step input in the ligand concentration; iii), same as in (ii) except in response to a rectangular pulse input (41); and iv), total Smad4 in the cytoplasm (30).

Fig. 3 *A* shows the predicted dynamics of total cellular (cytoplasmic + nuclear) Smad2 phosphorylation in response to a step input of 200 pM of TGF-β, compared to the corresponding experimental observations reported in Lo and Massague (43). The model prediction, especially the early response, shows remarkably good agreement with the data, even though its deviation from data becomes somewhat more pronounced with time after the peak.

A model prediction of the ratio of pSmad level to total Smad in response to a step input of 2 ng/ml of TGF-β is shown in Fig. 3 *B* compared to the experimental data of Lin et al. (41). Again, the agreement between model prediction and data is very good, with the prediction falling within the experimental error bars. How the ratio of pSmad2 level to total Smad2 responds to a short rectangular pulse of 2 ng/ml of TGF-β followed by TβRI kinase inhibitor SB431542 to block further phosphorylation (41) is shown in Fig. 3 *C*, where the model prediction is seen to match the data almost perfectly.

Finally, for cells induced by a step input of 2 ng/ml of TGF-β and treated by 20 μg of protein synthesis inhibitor, cycloheximide (30), Fig 3 *D* shows the agreement between the model prediction of cytoplasmic Smad4 response and the experimental data.

Overall, given that these are results of direct model predictions of four separate and independent experimental data sets, with no model parameter adjustments, we conclude that the model represents the dynamic behavior of the TGF-β signaling pathway quite well.

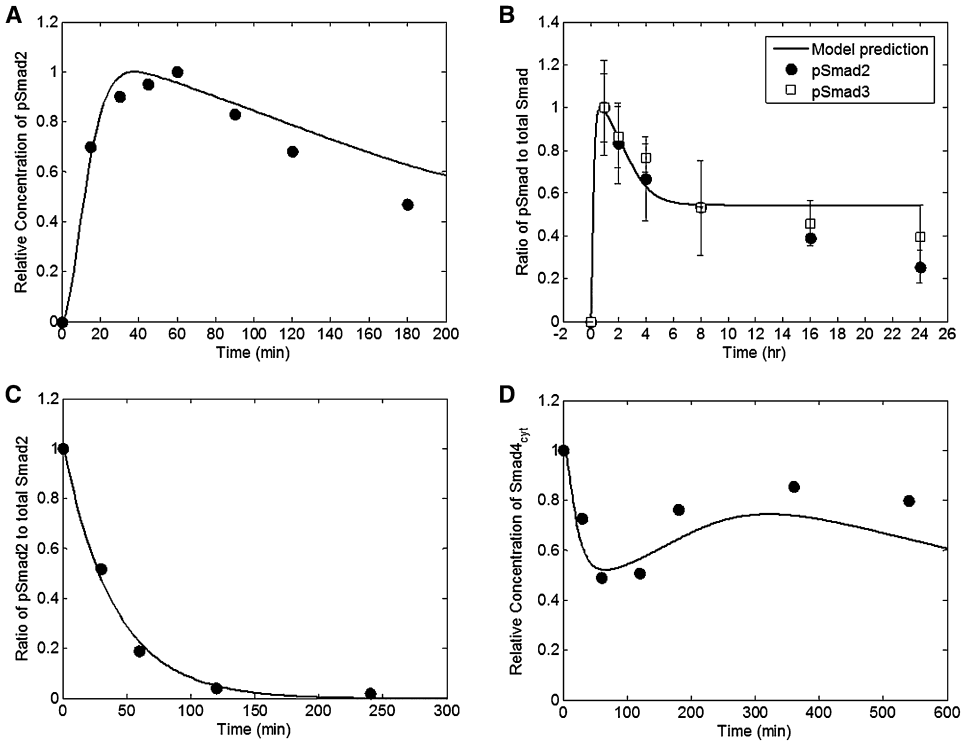

FIGURE 3 Model validation: (*A*) total cellular pSamd2 (43); (*B*) ratio of cellular pSmad2 to total Smad2 in response to the step input of TGF-β (41); (*C*) ratio of cellular pSmad2 to total Smad2 in response to the pulse input of TGF-β (41); (*D*) total cytoplasmic Smad4 (30). To simulate the effects of cycloheximide in (*D*), all rates of protein synthesis (k_{12syn}, k_{13syn}, k_{14syn}, and k_{15syn}) were set to zero.

Model analysis and simulation

In this section, we present results of computational ''experiments'' used to explore the dynamic behavior of the now-validated TGF-β signaling model. From among several signaling components in the pathway, we select phosphorylated Smad complex in the nucleus to represent the signaling activity of the TGF-β pathway because the expression of TGF-β-inducible genes is regulated by nuclear activated Smads. The premise is that such computational investigations into the dynamics of the TGF-β-induced Smad complex in the nucleus, under various conditions, will facilitate understanding and characterization of the TGF-β/Smad pathway; it also will provide clues regarding the role(s) of this pathway in tumor progression and metastasis. All simulations were carried out with the parameter values in Table 2, and step inputs of 80 pM of TGF-β, unless otherwise specified.

Model parameter sensitivity analysis

Although parameter sensitivity analysis has been shown to play an important role in parameter estimation, it also can be used to obtain insight into the model behavior itself. Specifically, sensitivity analysis carried out for the primary output of interest, nuclear pSmad2-Smad4 complex, will help us understand quantitatively which aspects of the pathway most affect the system behavior.

Fig. 4 shows normalized sensitivity coefficients as a function of time for the 10 most important parameters (parameters for which the maximum normalized sensitivity coefficient exceeds 0.5 in absolute value at any point in time). The most important features of this plot are summarized as follows: i), immediately after ligand stimulation, the output variable is strongly affected by four of this set of most sensitive parameters: in order of importance, these are k_{4a} (binding of Smad2 to active receptors), k_{3int} (internalization of receptor complexes), k_{7imp} (nuclear import of pSmad2-Smad4), and k_{2a} (complex formation of activated TβRII and TβRI); and ii), on the other hand, in the mid- to

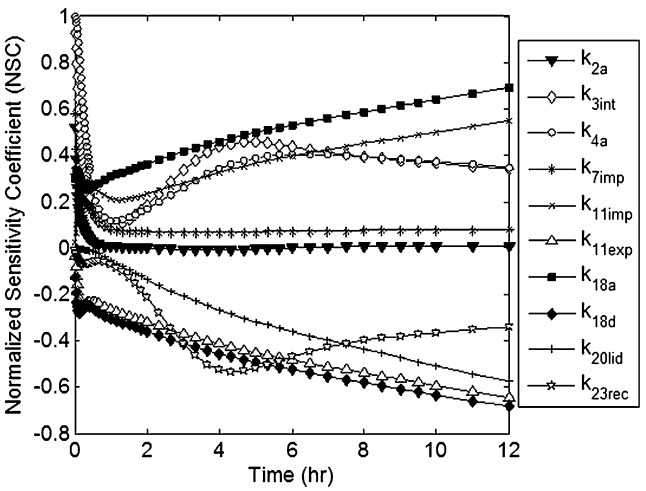

FIGURE 4 Model parameter sensitivities for select parameters with the greatest influence on phosphorylated Smad2-Smad4 complex in the nucleus. Parameters with maximum normalized sensitivity coefficients exceeding 0.5 in absolute value at any point in time are shown.

longer time interval after ligand stimulation, the following parameters become more important: in order of importance, these are k_{18a} (association of nuclear pSmad2 and Smad4), and k_{18d} (dissociation of nuclear pSmad2-Smad4), k_{11exp} (nuclear export of Smad4), k_{20lid} (ligand-induced degradation of pSmad2), k_{11imp} (nuclear import of Smad4), k_{23rec} (recycling of internalized receptor complexes), k_{3int} (internalization of receptor complexes), and k_{4a} (binding of Smad2 to active receptors).

These results have biologically important consequences. First, the high sensitivity coefficients of the receptor-related parameters (i.e., k_{2a}, k_{3int}, k_{4a}, and k_{23rec}) show that the system responses to TGF-β are highly dependent on the active state of the receptors. In particular, Fig. 4 shows that 45–60 min after TGF-β treatment, by which time nuclear pSmad2-Smad4 would have reached its peak activity (Fig. 2 *A*), the importance of the state of ligand-activated receptors on the species again increases. Considering that nuclear pSmad2-Smad4 complex loses its activity by dephosphorylation and is destroyed by proteasomal degradation, this result implies that to maintain accumulation of activated Smad complex in the nucleus, R-Smad must be continuously phosphorylated by active receptors. Taking into account that after ligand stimulation, free Smads in the cytoplasm are either still unphosphorylated or have been exported from the nucleus after undergoing dephosphorylation, this result reveals that the mechanism involving rephosphorylation of Smad plays a vital role in the nuclear accumulation of pSmad2-Smad4, especially at post peak times. To recycle Smad2 for rephosphorylation during active signaling, nuclear pSmad2 (either monomeric or heteromeric) must undergo dephosphorylation by phosphatases because only monomeric unphosphorylated Smad2 is capable of export from the nucleus to the cytoplasm so that the phosphorylated complexed form of Smad2 is trapped in the nucleus (32). Although the sensitivity analysis shows that nuclear pSmad2 complex is less sensitive to changes in the dephosphorylation step, this step is indispensable to the recycling of Smad2. To conclude, the parametric sensitivity analysis shows that the mechanisms for Smad2 recycling (i.e., phosphorylation-dephosphorylation-rephosphorylation) have a critical effect on the transcriptional activity of the signaling pathway.

The increasing nature of the sensitivity coefficients of k_{18a} and k_{18d} over time shows that both the formation of pSmad2-Smad4 complex in the nucleus and its dissolution are crucial for nuclear retention of these complexes. Our model has two sources of monomeric pSmad2 in the nucleus. One source is the dissociation of pSmad2-Smad4 complexes that are formed in the cytoplasm and then translocated to the nucleus; the other is nuclear entry of monomeric Smad2 that was phosphorylated in the cytoplasm. The former requires effective nuclear translocation of pSmad2-Smad4 complexes, as confirmed by the high sensitivity coefficient of the parameter k_{7imp}. Unlike other parameters, however, the effect of the nuclear import of activated Smad complexes is not significant over longer periods. On the other hand, considering that the importance of k_{18a} and k_{18d} increases over time (Fig. 4), it is likely that the latter source, the nuclear import of cytoplasmic monomeric pSmad2, also plays a vital role in the nuclear retention of pSmad2-Smad4 complexes. To confirm this, we computationally ''blocked'' the nuclear import of pSmad2-Smad4 complexes while allowing import of pSmad2 monomer, and then prevented nuclear import of pSmad2 monomer while allowing import of the complexed pSmad to study the effects of these ''blockades'' on the nuclear accumulation of active Smad complexes. Fig. 5 shows that the effect of blocking the nuclear import of cytoplasmic pSmad2-Smad4 complexes (i.e., the effect of nuclear complex formation between pSmad2 and Smad4) on nuclear retention of active Smad complexes is not trivial compared to the effect of preventing the nuclear entry of monomeric pSmad2. Taking the importance of Smad4 for nuclear complex formation into account, it is not surprising that the significance of nucleocytoplasmic shuttling of Smad4 (k_{11imp} and k_{11exp}) increases at longer times. Many biological ''models'' of the pathway mechanisms have neglected the nuclear entry of monomeric pSmads and the nuclear complex formation between Smad2 and Smad4, but this result argues strongly for their incorporation.

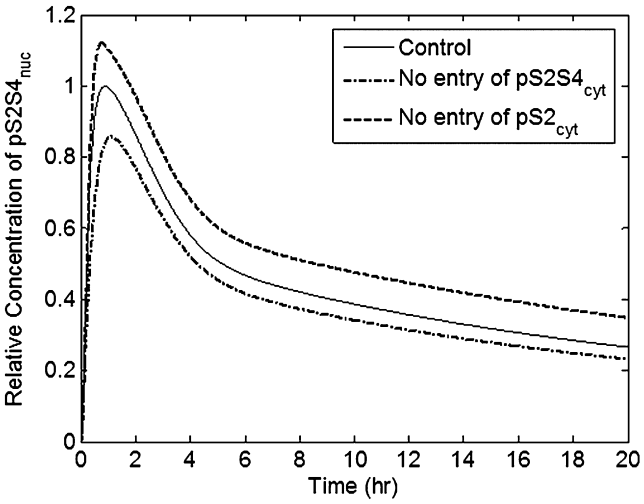

FIGURE 5 The effect of blocking translocation of monomeric pSmad2 (*dashed*, $k_{17imp} = 0$) or heteromeric pSmad2 (*dash dot*, $k_{7imp} = 0$).

The effect of Smad phosphorylation

As seen in previous sections, the nuclear accumulation of Smad2-Smad4 complexes is significantly affected by the dynamics of activated receptor complexes. To examine how variations in the active state of receptors influence the nuclear retention of pSmad2 complexes, we varied the rate of the binding between ligand-activated receptor complexes and Smad2 in the cytoplasm (k_{4a}) 10-fold, because the dynamics of the activated receptor complexes are ultimately reflected in the phosphorylation of Smad2 for downstream

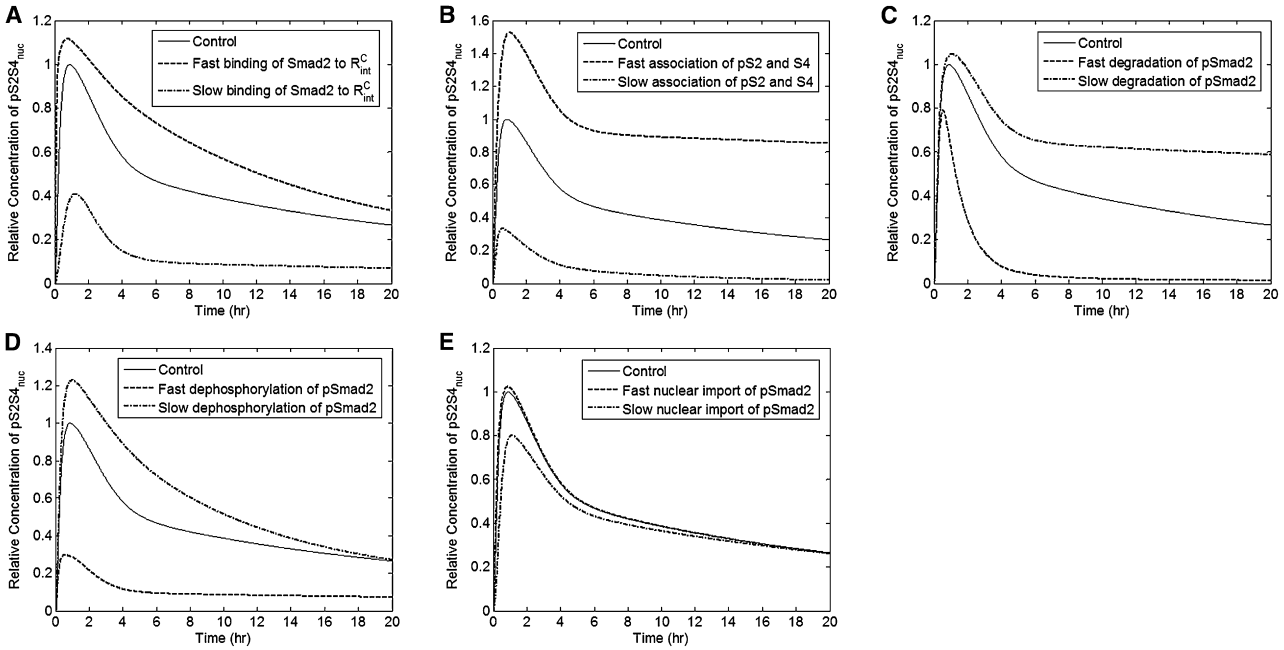

FIGURE 6 The effect of variations in the rate of (*A*) Smad2 phosphorylation, (*B*) nuclear pSmad2-Smad4 association, (*C*) pSmad2 degradation, (*D*) nuclear pSmad2 dephosphorylation, (*E*) and nuclear import of pSmad2 on the dynamics of nuclear pSmad2-Smad4 complex. Each indicated parameter value was increased (*dashed*) or decreased (*dash dot*) 10-fold.

signaling. Because it has been reported that Smad7, one of the inhibitory Smads, can bind to activated receptors in competition with R-Smads (29,52,53), this simulation may also provide insight into the inhibitory effect of Smad7 on TGF-β signaling. Fig. 6 *A* shows that when complex formation between ligand-activated receptors and Smad2 occurs more rapidly, more pSmad2 complexes are accumulated in the nucleus for a longer period, and the time to achieve peak accumulation of nuclear pSmad2 is shortened somewhat. Conversely, the slower binding of Smad2 to the receptors induces lower and slower accumulation of pSmad2 in the nucleus. These results suggest that regulation of the active state of the ligand-activated receptors and their complex formation with R-Smads may significantly affect the system responses to TGF-β through the nuclear retention of pSmad2 complexes in terms of the intensity and the duration of transcriptional activity.

The effect of nuclear Smad complex formation

We also investigated how Smad complex formation in the nucleus affects nuclear accumulation of activated Smad complexes, by varying the rate of association between nuclear pSmad2 and Smad4 (k_{18a}) 10-fold (Fig. 6 *B*). The results show that although rapid formation of the complex between nuclear pSmad2 and Smad4 induces prolonged and enhanced nuclear accumulation of pSmad2-Smad4 complex, slow binding of pSmad2 and Smad4 leads to shortened and attenuated retention of pSmad2 complex in the nucleus. Thus, these results imply that the nuclear complex formation step plays an important role in regulating the intensity and duration of TGF-β-targeted transcriptional activities through pSmad2 complexes. More importantly, the results imply that pSmad2 complex-mediated response to TGF-β stimulation may be attenuated significantly by competitive inhibition or by interference from other nuclear molecules that also have high affinity for either pSmad2 or Smad4. This inhibitory action ultimately gives rise to a significant reduction in the rate of association between these proteins. This conclusion is supported by a recent finding that a ubiquitous nuclear protein, transcriptional intermediary factor 1γ (TIF1γ), selectively binds receptor-phosphorylated Smad2/3 in competition with Smad4 (54,55). There is also the possibility that other molecules not yet identified may bind to either pSmad2 or Smad4 with high affinity; these putative molecules then would hamper complex formation between pSmad2 and Smad4. Taken together, these results show that the step of complex formation between pSmad2 and Smad4 is associated closely with modulation of TGF-β-induced signal patterns.

The effect of signal turn-off

Inactivation of ligand-activated R-Smads is crucial for controlling the extent of TGF-β effects. In our model, irreversible inactivation and termination of the pSmad2-mediated signals can be achieved in one of two ways: i), via ligand-induced ubiquitination and subsequent degradation by proteasomes; or ii), via dephosphorylation by inorganic phosphatases. We examined the effect of ligand-induced degradation of nuclear pSmad2 on the nuclear retention of pSmad2 complexes by changing the rate constant (k_{20lid})

10-fold. Fig. 6 *C* shows that slower degradation of pSmad2 results in higher and more sustained activity of nuclear pSmad2 complexes. On the other hand, when the rate of degradation is increased, the activity of pSmad2 complexes in the nucleus decreases more rapidly immediately after attaining its peak value, dropping almost to zero in the long term, hence resulting in transient dynamics. Taken together with the previous sensitivity analysis results, these simulations show that ligand-induced multi-ubiquitination via Smurf2 protein and subsequent degradation of activated Smad2 by proteasomes can play a vital role in regulating TGF-β-dependent transcription.

Similar system responses were obtained when the rates of pSmad2 dephosphorylation (k_{8dp} and k_{19dp}) were changed 10-fold (Fig. 6 *D*). When pSmad2 dephosphorylation occurred faster, the peak activity of nuclear pSmad2 complexes was noticeably reduced and the activity reached steady state more rapidly. However, the results show that variations in the dephosphorylation rates also changed the intensity of the response, but did not significantly affect the signal duration. This is because dephosphorylation by phosphatases can affect only the activity of nuclear Smads, and not the irreversible termination of the component itself. In other words, even though nuclear pSmads lose their activity by dephosphorylation, they can be rephosphorylated after exiting the nucleus, as long as the receptor activated signaling pathways remain active. These results therefore indicate that ligand-induced ubiquitination and subsequent proteasomal degradation can play an important role in regulating both the duration and intensity of Smad-mediated signal responses to TGF-β, whereas dephosphorylation may have a significant effect only on the signal intensity.

The effect of inhibiting nuclear import of active Smads

It has been reported that Smad activity can be regulated by diverse extracellular signal inputs through corresponding kinase pathways (2,6). One of the interactions between Smad and other pathways is achieved by direct phosphorylation of the linker region connecting the MH1 and MH2 domains of Smad proteins. This region is phosphorylated by endogenous mitogen-activated protein kinase, Ca^{2+}-calmodulin-dependent protein kinase II, and cyclin-dependent kinases. These inputs attenuate the nuclear accumulation and transcriptional activity of Smads, and negatively impact TGF-β signaling function. Although our model is limited in its ability to investigate all possible effects of crosstalk between TGF-β and other signaling pathways, still we are able to examine the effect of such input signals on the nuclear accumulation of Smads by directly varying the rate of nuclear import of TGF-β-activated Smads. Fig. 6 *E* shows that a large (10-fold) increase in the rates of nuclear translocation of both monomeric and complexed pSmad2 (k_{7imp} and k_{17imp}) does not have a pronounced effect on the nuclear retention of Smads. A 10-fold decrease in the rates resulted in a reduced response, but its effect is relatively insignificant when compared with the effects of variations in the parameter values of other important steps in the pathway. The immediate implication is that nuclear retention of Smads is relatively insensitive to crosstalk between Smad and other kinase pathways through phosphorylation of the Smad linker and consecutive inhibition of their entry to the nucleus.

TGF-β-dose-dependent responses

We examined the effect of various TGF-β concentrations well within the measured physiological extremes that surround cancer cells during cancer progression on the dynamics of the signaling system. Step inputs of four different concentrations of TGF-β (0.02, 0.2, 2, and 20 pM) were used to investigate the dose effects. These concentrations represent the range of measured concentrations of TGF-β produced by prostate cancer cells (0.4–4.8 pM) or bone marrow stromal cells (2.5–7 pM), or prostate fibroblasts (5 pM) (J. C. O'Connor and M. C. Farach-Carson, unpublished). All other conditions, including the initial conditions and kinetic parameters, remained the same. Fig. 7 *A* shows that as the TGF-β concentration increases, the activity of receptor complexes also increases and the peak activity time increases somewhat. Increases in TGF-β concentration also enhanced activity of receptor-activated Smad complexes and induced faster kinetics for active Smad complexes by allowing Smads to reach peak activity somewhat more rapidly (Fig. 7 *B*). For instance, although 0.02 pM of TGF-β induced maximum activity of Smads in 93 min, 20 pM of TGF-β resulted in peak activity of Smad in 54 min. Considering that activated Smad complexes in the nucleus regulate expression of TGF-β-target genes, these results show that an increase in the concentration of TGF-β may accelerate and enhance Smad-mediated cellular responses.

It is important to note that as the TGF-β concentration increases, the observed differences in the signaling activity diminish. For example, the response to a 2 pM stimulus is not significantly different from that for a 20 pM stimulus. This observation is true for both receptors and Smads. These results show that there is a saturation concentration of TGF-β above which Smad-mediated signaling responses within a cell no longer change. In other words, no matter how many bioactive TGF-β molecules are available in the extracellular space, each cell has a receptor-limited capacity to respond to them and consequently induce the corresponding signal responses.

In-silico mutations

How can cancer cells become resistant to the tumor-suppressor effects of TGF-β, but, at the same time, remain responsive to the tumor-promoter effects? We believe that differences between normal and cancerous signaling responses could offer some clues.

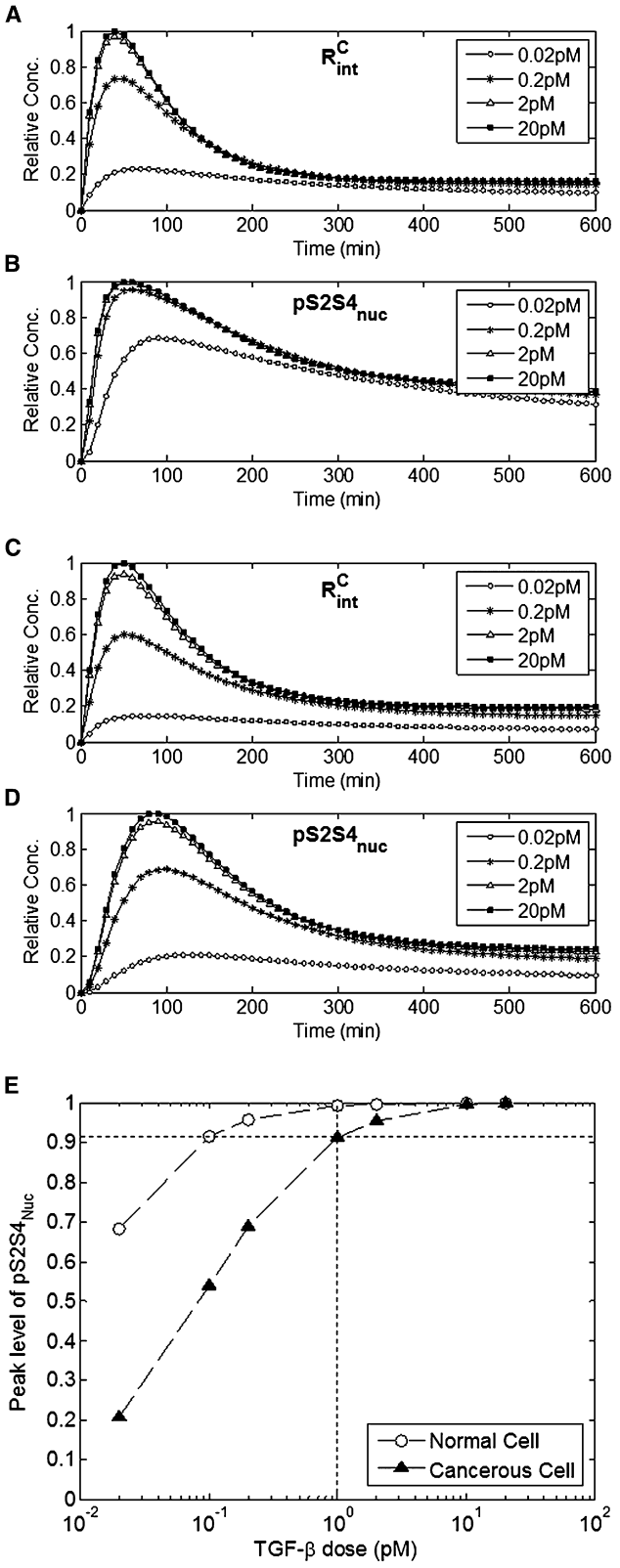

FIGURE 7 The effect of different concentrations of TGF-β on the dynamic responses of (*A*) internalized activated receptor complex and (*B*) activated Smad2-Smad4 complex in the nucleus under normal conditions, and (*C*) internalized activated receptor complex and (*D*) activated Smad2-Smad4 complex in the nucleus under cancerous conditions with 10-fold reduction in initial levels and protein synthesis rate constants of both Type I and Type II receptors. (*E*) Maximum responses of activated nuclear Smad2-Smad4 complex to different doses of TGF-β (0.02, 0.1, 0.2, 1, 2, 10, and 20 pM) in normal cells (*open circles*) and cancerous cells (*solid triangles*), respectively.

It is known that some signaling effectors of the TGF-β pathway are abnormally altered in many human tumors (56). Specifically, aberrant alterations such as mutations, deletions, and downregulation of Type I and/or Type II receptors are observed most frequently in a variety of human cancers including prostate, breast, ovarian, bladder, gastric, and pancreatic cancer. We have therefore investigated the effect on the TGF-β signaling system of some of these common abnormal alterations in receptors, using a 10-fold reduction in the initial levels and production rate of both Type I and Type II receptors to represent cancerous conditions.

First, Fig. 7, *C* and *D*, show the TGF-β dose-dependent responses for cancerous cells, corresponding to what was shown earlier in Fig. 7, *A* and *B*, for normal cells. Although a comparison of Fig. 7, *A* and *C*, shows only slight differences in the relative activity of receptor complexes for normal and cancerous cells, the situation is different with the nuclear Smad-mediated activity. Fig. 7 *E* indicates that the amount of TGF-β needed to produce saturated Smad-mediated response in cancer cells is far higher than that in healthy cells. Specifically, whereas the response for normal cells is essentially saturated with 0.1 pM of TGF-β (with higher doses producing essentially the same response) at least 1 pM of TGF-β is required before the Smad-mediated response begins to approach saturation. This is, of course, a direct effect of the reduction in the number of functional receptors in cancer cells (56) that renders the them less responsive to TGF-β stimulation. But this finding also indicates an important characteristic of cancerous cells: to elicit nuclear Smad-mediated activity generally requires more TGF-β than normal.

Next, a head-to-head comparison of normal versus cancerous cell responses shows some very interesting features. Fig. 8 *A* shows that when the level of functional receptors is very low, the activity of ligand-activated receptor complexes (in response to a step of 2 ng/mL, or 80 pM TGF-β) is significantly attenuated compared to that in the normal system. Specifically, the peak level of active receptors in the cancerous system plunges by an astounding 92%. Thus, even though the dose-response characteristics of active receptors are essentially similar for both classes of cells, the actual peak level attained is significantly lower for cancer cells. Once again, this is consistent with what one would expect from cells having fewer functional receptors (56).

Not surprisingly, due to the correlation between active receptors and nuclear pSmads, Fig. 8 *B* shows that the sharp drop in the level of functional receptors in cancer cells leads to a marked decrease in the activity of nuclear pSmad

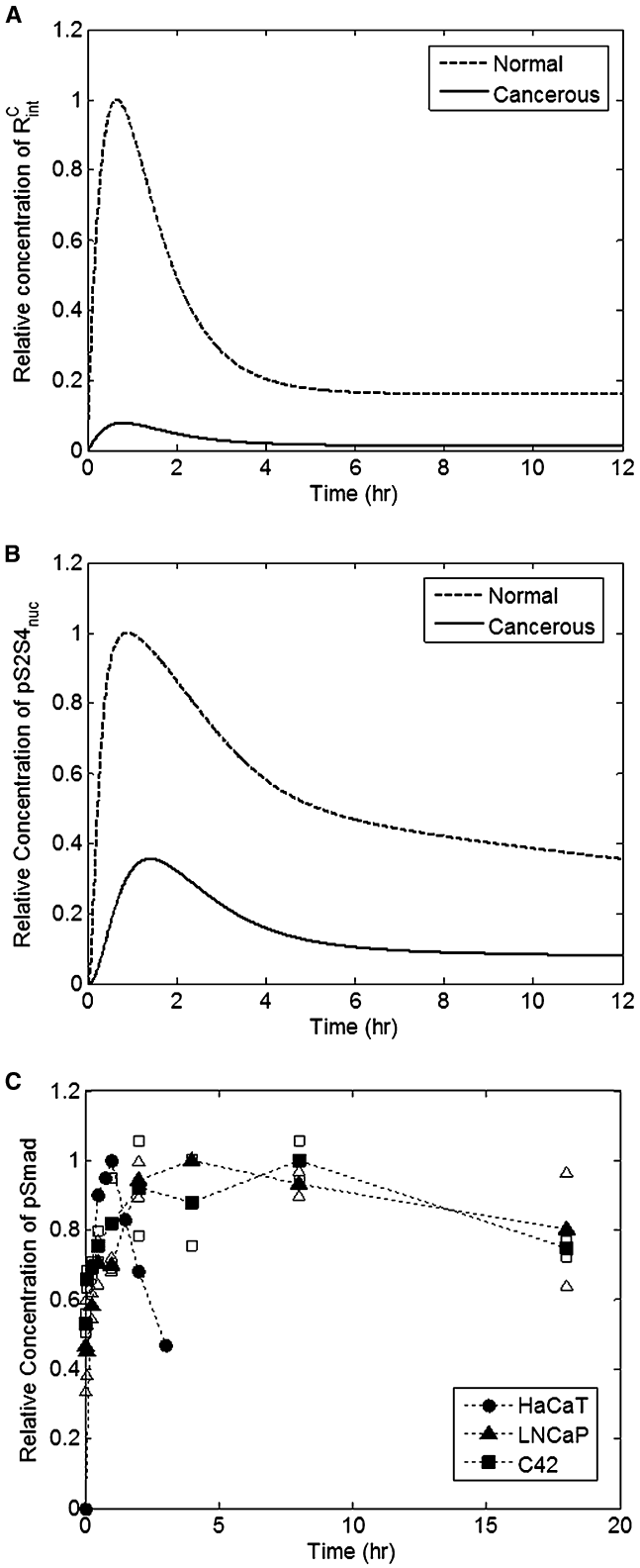

FIGURE 8 In silico mutation results. Responses of (*A*) internalized activated receptor complex and (*B*) nuclear pSmad-Smad4 complex to 10-fold reduction in initial levels and protein synthesis rate constants of both Type I and Type II receptors. (*C*) Temporal profiles of phosphorylated Smad2 in HaCaT cells (*circles*, from Lo and Massague (43)), LNCaP cells (*triangles*, our experiments), and C4-2 cells (*squares*, our experiments) in response to 200 pM (for *A*) or 400 pM (for *B* and *C*) of TGF-β. The open triangles and squares represent the maximum and minimum of the data at each time point; the solid squares and triangles denote the corresponding average values. All data points were normalized with respect to the maximum intensity value of pSmad2 of each profile.

complexes. Compared to the normal cell response, the peak activity of nuclear pSmad complexes in cancer cells was reduced by 65%, with the steady-state activity also remaining comparatively low.

Interestingly, a reduction in the level of receptors also slowed nuclear pSmad responses. Although nuclear pSmads in the normal system reached maximum activity in 55 min, their activity under a cancerous condition peaked at 86 min. These results are consistent with our own experimental observations of Smad2 phosphorylation in some prostate cancer cell lines (i.e., LNCaP and C4-2) as shown in Fig. 8 *C*. (A separate assay, not shown, confirmed that both LNCaP and C4-2 cells have low levels of TGF-β Type I and Type II receptor proteins.) Whereas peak activity of phosphorylated R-Smads is attained ~1 h after ligand addition in cells with intact TGF-β signaling machinery (43), the metastatic prostate cancer cells with reduced functional receptors showed peak activity much later, as a result of the slower dynamics of activated Smad2 (Fig. 8 *C*). Although the kinetics of pSmad2 in the cancer cells could potentially be affected by many factors (e.g., cancer types, cell lines, cell culture conditions, etc.), our simulation and experimental results reveal that reduction in the receptor levels, a notable phenotypic difference between normal and cancer cells, is associated closely with differences in the dynamic behavior of the pathway.

Taken together, these results indicate generally that a reduction in the level of functional TGF-β receptors in cancer cells may lead to attenuated and slower TGF-β-stimulated signaling responses via Smad2. The specific implications of the model predictions in Figs. 7 and 8 show some potentially important findings about TGF-β and cancer cells: i), cancer cells require higher than normal levels of TGF-β to elicit significantly attenuated (and much slower) nuclear Smad-mediated activity; and ii), even the increased levels of TGF-β will never be able to produce Smad-mediated responses that will be anywhere close to normal because of the saturation effect shown in Fig. 7 *D*. These characteristics may have significant implications for cancer therapies that are based on targeting TGF-β.

Hypotheses on the dual role of TGF-β

As seen above, the dynamic patterns of major signaling components in cancer cells in response to TGF-β may be quite different from those in normal cells. Such differences may provide clues regarding the role of TGF-β—tumor suppressor or tumor enhancer—during cancer progression. Here, we postulate four testable nonmutually exclusive

hypotheses arising from our foregoing analysis of the system dynamics.

Hypothesis 1: different thresholds for gene expression

As shown above via simulation, cancer cells have attenuated TGF-β-stimulated Smad pathway responses. Such cells have been confirmed experimentally to be resistant to the antiproliferative effect of TGF-β, while showing typical prooncogenic responses. Such behavior may be explained in part by the following ''threshold hypothesis'': in response to TGF-β, growth-inhibitory genes require higher threshold levels of nuclear Smad activity for their expression than genes associated with prooncogenic and prometastatic effects. In other words, under normal conditions, or in the early stage of cancer progression, the antiproliferative responses to TGF-β are predominant over prooncogenic responses. This is because the transcriptional activity of nuclear pSmad is high enough to induce anti-growth gene expression. However, as cancer progresses, this transcriptional activity may decline significantly and thereby hardly exceed the threshold necessary for the expression of growth-inhibition genes. Meanwhile, genes related to tumor-promoting effects may be relatively insensitive to the attenuation of the transcriptional activity by Smads, so that the expression of such genes remains approximately unchanged even under cancerous conditions. As a consequence, the dominance of tumor suppressor genes over the tumor-promoter genes may be blunted in cancer cells. This hypothesis is supported in part by previous experimental observations that cells with reduced TGF-β receptor function showed resistance to the antiproliferative effect of TGF-β, whereas other TGF-β responses were not significantly affected (51,57–59). We believe that further investigation into differences in the temporal profiles of gene expression and thresholds of anti-growth and prooncogenic genes induced by TGF-β will provide some clues regarding the putative dual effects of TGF-β.

Hypothesis 2: fast degradation of signaling components

It has been suggested that the duration of TGF-β/Smad signaling is a critical determinant for regulating specificity of cellular responses (60). For example, Nicolas and Hill (51) reported that normal epithelial cells (HaCaT and Colo-357) with sustained retention of active Smad in the nucleus (>6 h after TGF-β addition) are sensitive to growth inhibition by TGF-β. In contrast, pancreatic cancer cells (PT45 and Panc-1) showing transient nuclear retention of active Smads (1–2 h after TGF-β treatment) preferentially evade the growth-inhibitory effects of TGF-β, with no changes to other responses. Thus, it seems likely that the expression profile of TGF-β-inducible genes required for cell cycle arrest may differ depending on the dynamic patterns of nuclear pSmads. Taking into account that such pancreatic cancer cell lines contain low levels of TGF-β Type I receptor protein (51), one may be tempted to conclude that the reduction in receptor levels is responsible for driving the transient accumulation of pSmads in the nucleus to induce alteration in the expression profiles of the anti-growth genes. However, reduced levels of receptors may not be the only factor leading to the experimentally observed short-term signal response to TGF-β. We hypothesize that such transient dynamic behavior of nuclear pSmads results from not only a reduction in receptor levels but also from other mechanisms, especially mechanisms associated with rapid degradation of major signaling components in the pathway. We have already seen responses become transient when the rate of pSmad2 degradation increased (Fig. 6 *C*). Alterations in the mechanism(s) involved in degradation of pSmad2 during cancer progression may therefore account for producing transient signal responses to TGF- β.

It also is possible that Smad4 may be a major target for rapid degradation. Western blot analysis (51) showed that whereas the activity of Smad4 is sustained in normal cells during active signaling, Smad4 from nuclear extracts of pancreatic cancer cells shows fairly transient dynamics. We suspect that the transient dynamics of Smad4 in cancer cells result from an expedited degradation process for Smad4 (Fig. 9 *A*). To confirm that such a rapid degradation of these two major signaling components, pSmad2 and Smad4, contributes to the transient dynamics of nuclear pSmad2 under cancerous conditions, we carried out simulations with 10-fold increases in the rate constants for either pSmad2 or Smad4 or both under cancerous conditions where the level of receptors is reduced 10-fold. Fig. 9 *B* shows that the increased degradation rate of pSmad2 and/or of Smad4, along with decreased expression of receptors, leads to more attenuated and transient dynamics of activated Smads, compared to the response to a decrease in the level of the receptors alone. This hypothesis is corroborated by previous findings that in response to TGF-β, tumor cells show increased production of proteases and downregulation of the protease inhibitors, leading to rapid degradation of signaling components; these features are not observed in normal cells (61). Further investigations into changes in the degradation mechanisms of the signaling components in the pathway during cancer progression may therefore be important in understanding the apparently contradictory roles of TGF-β.

Hypothesis 3: competitive inhibition by nuclear binding partner of pSmad

Our sensitivity analysis has shown that association and dissociation between pSmad2 and Smad4 in the nucleus critically affect nuclear accumulation of pSmad2-Smad4 complexes in terms of signal intensity and duration. In particular, Fig. 6 *B* shows that retardation of nuclear complex formation of pSmad2 with Smad4 leads to attenuated and transient signal responses. We hypothesize that one possible factor in the sluggishness of pSmad2-Smad4 complex formation is competitive inhibition by other binding partners of

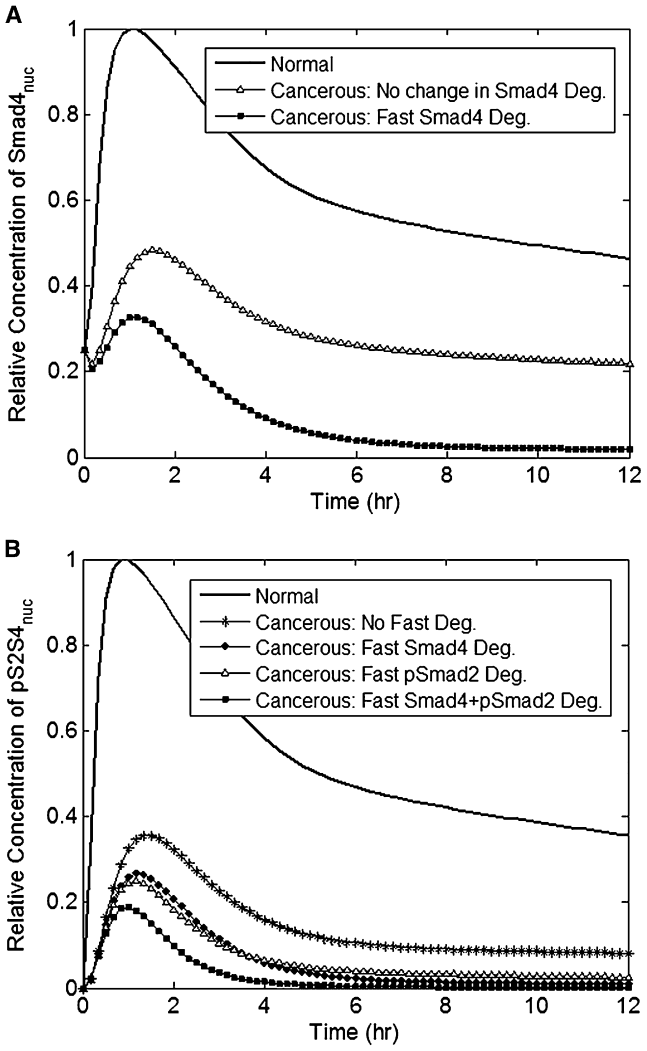

FIGURE 9 Model predictions for (*A*) nuclear Smad4 and (*B*) nuclear pSmad2-Smad4 complex on TGF-β stimulation (80 pM) under cancerous conditions; 10-fold reduction in the initial levels and the protein synthesis rate constants of both Type I and Type II receptors, and 10-fold increase in rates of degradation of either Smad4 (*A*, *squares*; *B*, *diamonds*) or pSmad2 (*B*, *triangles*) or both (*B*, *squares*).

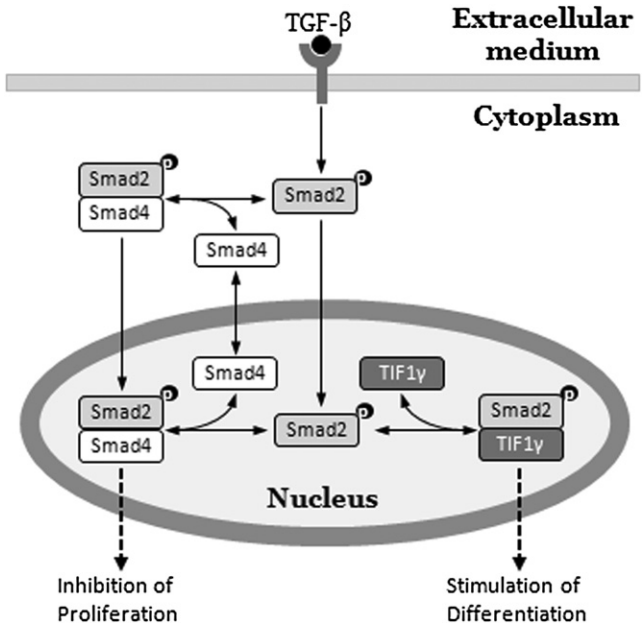

FIGURE 10 Alternative TGF-β-induced responses determined by nuclear pSmad2-binding partners. Whereas Smad4 forms transcriptional complexes with receptor-phosphorylated Smad2/3 and mediates antiproliferative responses, TIF1γ specifically recognizes receptor-activated Smad2/3 and mediates differentiation of hematopoietic stem/progenitor cells. (Adapted from He et al. (54)).

ligand-activated Smad in the nucleus, apart from Smad4. This is supported by a recent finding that a ubiquitous nuclear protein, TIF1γ, can selectively bind to ligand-activated Smad2/3, competing with Smad4 (54), a schematic diagram of which is shown in Fig. 10. This study suggests the possible existence of hitherto unidentified binding partners that show high affinity for receptor-phosphorylated Smad2.

Such binding partners may inhibit not only complex formation between pSmad2 and Smad4, but also may mediate cellular responses different from those mediated by Smad4. The same study (54) showed that in human hematopoietic progenitor cells, the binding of receptor-phosphorylated Smad2/3 to Smad4 mediates inhibition of proliferation, whereas complex formation of pSmad2/3 with TIF1γ mediates differentiation in response to TGF-β. This result strongly suggests the possibility that the Smad pathway can mediate a variety of cellular responses through its branch pathways, depending on nuclear binding partners of TGF-β-induced R-Smads. In particular, if such putative binding partners can mediate cellular responses contradictory to those mediated by Smad4, this may explain the dual role of TGF-β during cancer progression. Suppose that during cancer progression the rate of complex formation between R-Smads and Smad4 slows because of either lower affinity between those molecules or because of higher affinity between R-Smads and other binding proteins, due to conformational changes by mutations or for other reasons. Suppose as well that such binding proteins strongly mediate tumor-promoting responses such as EMT, invasion, and survival. A decreased rate of complex formation between pSmads and Smad4 in the nucleus can lead to an increased number of free nuclear pSmads that can bind to other nuclear partners; this makes for a higher probability of complex formation between pSmads and other partners. Considering that slow association of pSmad2 with Smad4 leads to attenuated and transient responses (primarily tumor-suppressive ones), increased complex formation between pSmad2 and potential binding factors may cause higher and prolonged tumor-promoting responses. Consequently, in cancers, an imbalance between tumor-suppressing responses by Smad4 and tumor-promoting responses by potential binding factors may explain the paradox of TGF-β.

Hypothesis 4: a TGF-β control system

Although the aforementioned hypotheses deal with potential intracellular mechanisms by which the tumor suppressor effects of TGF-β are lessened in cancer, the question remains why the levels of TGF-β are unusually high in the primary tumor and plasma of cancer patients with poor prognosis, given that this cytokine is primarily a tumor suppressor/growth inhibitor? The observed correlation between high levels of TGF-β and poor prognosis has often led many researchers to reach a consensus that the elevated TGF-β level is an indication that TGF-β is a tumor promoter; accordingly, significant efforts have been devoted to developing TGF-β inhibitors as cancer therapy (62).

However, our dose-response results provide a potential alternative perspective of this clinical observation, i.e., that increased levels of TGF-β correlate with poor prognosis does not mean that the former causes the latter. First, the simulations results in Fig. 7 show that cancer cells may require higher than normal levels of TGF-β to elicit nuclear Smad-mediated activity. If nuclear Smad-mediated activity is necessary for effective tumor suppression/growth inhibition, then this result is consistent with the established fact that, as a result of loss of functional TGF-β receptors, cancer cells become resistant to the growth inhibitory effect of TGF-β (63). Now, from a control theory perspective, this phenomenon seems to be analogous to that of a temperature control problem in an exothermic nuclear reactor supplied with a cooling jacket. If the cooling jacket surrounding the reactor becomes encrusted with accumulated deposits from the water supply, the reactor will become less responsive to the cooling water, and increasing amounts will be needed to cool the reactor. As the reactor walls become even less responsive with time, an automatic temperature controller will call for increasing amounts of cooling water even as the temperature continues to rise; the rising temperature will cause more nuclear reaction, which in turn will cause the temperature to rise even further. Eventually meltdown will occur when the cooling is no longer able to keep up. A postaccident analysis of these circumstances will show the increasing temperature accompanied by increasing cooling water flow rate, giving the illusion that the cooling water caused the temperature to increase. However, common sense will dismiss this as invalid because the role of cooling water in reactor temperature control is well understood.

We therefore hypothesize that there exists a cellular control system that uses the tumor suppressor ligand, TGF-β, to achieve its objective of regulating cell growth (64). This control system functions effectively in normal cells because they are responsive to this ligand. But as a direct consequence of TGF-β resistance in tumor cells, the still-intact control system must now secrete more of this ligand in a futile attempt to achieve the level of tumor suppression attainable with normal, responsive cells. Thus, the observed increased level of TGF-β is a consequence of this acquired TGF-β resistance exhibited by the cancer cells, not the cause. The correlation between increased levels of TGF-β and poor prognosis has been inadvertently misconstrued as causality, creating the apparent paradox. The clinically observed increased TGF-β level is therefore not an indication that the tumor suppressor role of TGF-β has changed fundamentally; rather, with this control system hypothesis, it is consistent with TGF-β's role as a tumor suppressor that its level should increase in an attempt to elicit normal responses from a tumor that is becoming increasingly resistant to the cytokine.

If this hypothesis is true, the consequences for how TGF-β ligand and TGF-β receptors are used as therapeutic agents will be significant. Specifically, it will mean that the current approach of targeting TGF-β ligand therapeutically may have to be abandoned in favor of re-sensitizing the cells to the tumor suppressive effect of the TGF-β, similar to treatment for diabetes mediated by prolonged insulin-resistance (65).

We intend to investigate and test each of these hypotheses in subsequent studies.

CONCLUSIONS

In this work we have presented a mathematical description of the TGF-β signaling pathway that is more comprehensive and more realistic than the previous computational models; it integrates extracellular signal transduction and intracellular signal transmission, and includes some reaction mechanisms modified from previous models to be better aligned with current knowledge of the TGF-β pathway. The model, which shows good fit to multiple sources of experimental data, simultaneously, was also validated against several totally different, independent sets of data from different sources, without adjusting any model parameters. Extensive analysis of the model (parametric sensitivity and model predictions under various physiological conditions) has provided insight into basic characteristics of the TGF-β signaling system.

We believe that our model also yields new insights into the relationship between ligand stimulation and corresponding responses via binding of TGF-β to its receptor at the cell surface and the activation of downstream effectors in the signaling cascade; it also yields new insights into molecular TGF-β-induced response characteristics that distinguish between normal and cancer cells. Furthermore, these results provide some clues that may be helpful in unraveling long-standing questions about the seemingly contradictory roles of TGF-β during cancer progression. However, the model still has some limitations. We plan to expand the current model first to incorporate the effect of crosstalk among other important signaling cascades, and later gene expression mechanisms. Our future plans also include focusing on prostate cancer (PCa), customizing this computational model for the PCa cell lines of the LNCaP human prostate cancer progression model available in our laboratory, and using the models for a model-guided experimental study of the

role of TGF-β during PCa progression and testing the four hypotheses postulated above.

We express our appreciation to Dr. John O'Connor for sharing his thesis data including the concentrations of TGFβ1 secreted by various prostate cancer and stromal cells.

This work was supported by Institute for Multiscale Modeling of Biological Interactions (IMMBI) funded by the Department of Energy, and by the Department of Defense grant PC050554. Additional work was supported by National Institutes of Health/National Cancer Institute P01 CA098912, the University of Delaware Research Foundation and the National Institutes of Health INBRE P20RR016472.

REFERENCES

1. Massague, J. 1998. TGF-β signal transduction. *Annu. Rev. Biochem.* 67:753–791.
2. Massague, J., and R. R. Gomis. 2006. The logic of TGFβ signaling. *FEBS Lett.* 580:2811–2820.
3. Shi, Y., and J. Massague. 2003. Mechanisms of TGF-β signaling from cell membrane to the nucleus. *Cell.* 113:685–700.
4. Massague, J. 2000. How cells read TGF-β signals. *Nat. Rev. Mol. Cell Biol.* 1:169–178.
5. Itoh, S., F. Itoh, M. J. Goumans, and P. Ten Dijke. 2000. Signaling of transforming growth factor-β family members through Smad proteins. *Eur. J. Biochem.* 267:6954–6967.
6. Feng, X. H., and R. Derynck. 2005. Specificity and versatility in TGF-β signaling through Smads. *Annu. Rev. Cell Dev. Biol.* 21:659–693.
7. Wikstrom, P., P. Stattin, I. Franck-Lissbrant, J. E. Damber, and A. Bergh. 1998. Transforming growth factor β1 is associated with angiogenesis, metastasis, and poor clinical outcome in prostate cancer. *Prostate.* 37:19–29.
8. Shariat, S. F., J. H. Kim, B. Andrews, M. W. Kattan, T. M. Wheeler, et al. 2001. Preoperative plasma levels of transforming growth factor β(1) strongly predict clinical outcome in patients with bladder carcinoma. *Cancer.* 92:2985–2992.
9. Kattan, M. W., S. F. Shariat, B. Andrews, K. Zhu, E. Canto, et al. 2003. The addition of interleukin-6 soluble receptor and transforming growth factor β1 improves a preoperative nomogram for predicting biochemical progression in patients with clinically localized prostate cancer. *J. Clin. Oncol.* 21:3573–3579.
10. Elliott, R. L., and G. C. Blobe. 2005. Role of transforming growth factor β in human cancer. *J. Clin. Oncol.* 23:2078–2093.
11. Wakefield, L. M., and A. B. Roberts. 2002. TGF-β signaling: positive and negative effects on tumorigenesis. *Curr. Opin. Genet. Dev.* 12:22–29.
12. Pardali, K., and A. Moustakas. 2007. Actions of TGF-β as tumor suppressor and pro-metastatic factor in human cancer. *Biochim. Biophys. Acta.* 1775:21–62.
13. Vilar, J. M., R. Jansen, and C. Sander. 2006. Signal processing in the TGF-β superfamily ligand-receptor network. *PLoS Comput Biol.* 2:e3.
14. Clarke, D. C., M. D. Betterton, and X. Liu. 2006. Systems theory of Smad signalling. *Syst. Biol. (Stevenage).* 153:412–424.
15. Melke, P., H. Jonsson, E. Pardali, P. Ten Dijke, and C. Peterson. 2006. A rate equation approach to elucidate the kinetics and robustness of the TGF-β pathway. *Biophys J.* 91:4368–4380.
16. Zi, Z., and E. Klipp. 2007. Constraint-based modeling and kinetic analysis of the Smad dependent TGF-β signaling pathway. *PLoS ONE.* 2:e936.
17. Schmierer, B., A. L. Tournier, P. A. Bates, and C. S. Hill. 2008. Mathematical modeling identifies Smad nucleocytoplasmic shuttling as a dynamic signal-interpreting system. *Proc. Natl. Acad. Sci. USA.* 105:6608–6613.
18. Mitchell, H., A. Choudhury, R. E. Pagano, and E. B. Leof. 2004. Ligand-dependent and -independent transforming growth factor-β receptor recycling regulated by clathrin-mediated endocytosis and Rab11. *Mol. Biol. Cell.* 15:4166–4178.
19. Di Guglielmo, G. M., C. Le Roy, A. F. Goodfellow, and J. L. Wrana. 2003. Distinct endocytic pathways regulate TGF-β receptor signalling and turnover. *Nat. Cell Biol.* 5:410–421.
20. Inman, G. J., F. J. Nicolas, and C. S. Hill. 2002. Nucleocytoplasmic shuttling of Smads 2, 3, and 4 permits sensing of TGFβ receptor activity. *Mol. Cell.* 10:283–294.
21. Hayes, S., A. Chawla, and S. Corvera. 2002. TGFβ receptor internalization into EEA1-enriched early endosomes: role in signaling to Smad2. *J. Cell Biol.* 158:1239–1249.
22. Penheiter, S. G., H. Mitchell, N. Garamszegi, M. Edens, J. J. Dore, Jr., et al. 2002. Internalization-dependent and -independent requirements for transforming growth factor β receptor signaling via the Smad pathway. *Mol. Cell. Biol.* 22:4750–4759.
23. Funaba, M., and L. S. Mathews. 2000. Identification and characterization of constitutively active Smad2 mutants: evaluation of formation of Smad complex and subcellular distribution. *Mol. Endocrinol.* 14:1583–1591.
24. Wu, J. W., R. Fairman, J. Penry, and Y. Shi. 2001. Formation of a stable heterodimer between Smad2 and Smad4. *J. Biol. Chem.* 276:20688–20694.
25. Wu, J. W., M. Hu, J. Chai, J. Seoane, M. Huse, et al. 2001. Crystal structure of a phosphorylated Smad2. Recognition of phosphoserine by the MH2 domain and insights on Smad function in TGF-β signaling. *Mol. Cell.* 8:1277–1289.
26. Chacko, B. M., B. Y. Qin, A. Tiwari, G. Shi, S. Lam, et al. 2004. Structural basis of heteromeric Smad protein assembly in TGF-β signaling. *Mol. Cell.* 15:813–823.
27. Kawabata, M., H. Inoue, A. Hanyu, T. Imamura, and K. Miyazono. 1998. Smad proteins exist as monomers in vivo and undergo homo- and hetero-oligomerization upon activation by serine/threonine kinase receptors. *EMBO J.* 17:4056–4065.
28. Jayaraman, L., and J. Massague. 2000. Distinct oligomeric states of SMAD proteins in the transforming growth factor-β pathway. *J. Biol. Chem.* 275:40710–40717.
29. Massague, J., J. Seoane, and D. Wotton. 2005. Smad transcription factors. *Genes Dev.* 19:2783–2810.
30. Pierreux, C. E., F. J. Nicolas, and C. S. Hill. 2000. Transforming growth factor β-independent shuttling of Smad4 between the cytoplasm and nucleus. *Mol. Cell. Biol.* 20:9041–9054.
31. Reguly, T., and J. L. Wrana. 2003. In or out? The dynamics of Smad nucleocytoplasmic shuttling. *Trends Cell Biol.* 13:216–220.
32. Schmierer, B., and C. S. Hill. 2005. Kinetic analysis of Smad nucleocytoplasmic shuttling reveals a mechanism for transforming growth factor β-dependent nuclear accumulation of Smads. *Mol. Cell. Biol.* 25:9845–9858.
33. Nicolas, F. J., K. De Bosscher, B. Schmierer, and C. S. Hill. 2004. Analysis of Smad nucleocytoplasmic shuttling in living cells. *J. Cell Sci.* 117:4113–4125.
34. Xu, L., Y. Kang, S. Col, and J. Massague. 2002. Smad2 nucleocytoplasmic shuttling by nucleoporins CAN/Nup214 and Nup153 feeds TGFβ signaling complexes in the cytoplasm and nucleus. *Mol. Cell.* 10:271–282.
35. De Bosscher, K., C. S. Hill, and F. J. Nicolas. 2004. Molecular and functional consequences of Smad4 C-terminal missense mutations in colorectal tumour cells. *Biochem. J.* 379:209–216.
36. Fink, S. P., D. Mikkola, J. K. Willson, and S. Markowitz. 2003. TGF-β-induced nuclear localization of Smad2 and Smad3 in Smad4 null cancer cell lines. *Oncogene.* 22:1317–1323.
37. Xu, L., C. Alarcon, S. Col, and J. Massague. 2003. Distinct domain utilization by Smad3 and Smad4 for nucleoporin interaction and nuclear import. *J. Biol. Chem.* 278:42569–42577.

38. Xu, L., and J. Massague. 2004. Nucleocytoplasmic shuttling of signal transducers. *Nat. Rev. Mol. Cell Biol.* 5:209–219.

39. Kurisaki, A., S. Kose, Y. Yoneda, C. H. Heldin, and A. Moustakas. 2001. Transforming growth factor-β induces nuclear import of Smad3 in an importin-β1 and Ran-dependent manner. *Mol. Biol. Cell.* 12:1079–1091.

40. Xiao, Z., R. Latek, and H. F. Lodish. 2003. An extended bipartite nuclear localization signal in Smad4 is required for its nuclear import and transcriptional activity. *Oncogene.* 22:1057–1069.

41. Lin, X., X. Duan, Y. Y. Liang, Y. Su, K. H. Wrighton, et al. 2006. PPM1A functions as a Smad phosphatase to terminate TGFβ signaling. *Cell.* 125:915–928.

42. Schmierer, B., and C. S. Hill. 2007. TGFβ-SMAD signal transduction: molecular specificity and functional flexibility. *Nat. Rev. Mol. Cell Biol.* 8:970–982.

43. Lo, R. S., and J. Massague. 1999. Ubiquitin-dependent degradation of TGF-β-activated Smad2. *Nat. Cell Biol.* 1:472–478.

44. Lin, X., M. Liang, and X. H. Feng. 2000. Smurf2 is a ubiquitin E3 ligase mediating proteasome-dependent degradation of Smad2 in transforming growth factor-β signaling. *J. Biol. Chem.* 275:36818–36822.

45. Zhang, Y., C. Chang, D. J. Gehling, A. Hemmati-Brivanlou, and R. Derynck. 2001. Regulation of Smad degradation and activity by Smurf2, an E3 ubiquitin ligase. *Proc. Natl. Acad. Sci. USA.* 98:974–979.

46. Wan, M., X. Cao, Y. Wu, S. Bai, L. Wu, et al. 2002. Jab1 antagonizes TGF-β signaling by inducing Smad4 degradation. *EMBO Rep.* 3:171–176.

47. Schoeberl, B., C. Eichler-Jonsson, E. D. Gilles, and G. Muller. 2002. Computational modeling of the dynamics of the MAP kinase cascade activated by surface and internalized EGF receptors. *Nat. Biotechnol.* 20:370–375.

48. Wakefield, L. M., D. M. Smith, T. Masui, C. C. Harris, and M. B. Sporn. 1987. Distribution and modulation of the cellular receptor for transforming growth factor-β. *J. Cell Biol.* 105:965–975.

49. Wilkinson, K. D. 2004. Quantitative Analysis of Protein-Protein Interactions. Humana Press, Totowa, New Jersey.

50. Birtwistle, M. R., M. Hatakeyama, N. Yumoto, B. A. Ogunnaike, J. B. Hoek, et al. 2007. Ligand-dependent responses of the ErbB signaling network: experimental and modeling analyses. *Mol. Syst. Biol.* 3:144.

51. Nicolas, F. J., and C. S. Hill. 2003. Attenuation of the TGF-β-Smad signaling pathway in pancreatic tumor cells confers resistance to TGF-β-induced growth arrest. *Oncogene.* 22:3698–3711.

52. Nakao, A., M. Afrakhte, A. Moren, T. Nakayama, J. L. Christian, et al. 1997. Identification of Smad7, a TGFβ-inducible antagonist of TGF-β signalling. *Nature.* 389:631–635.

53. Hayashi, H., S. Abdollah, Y. Qiu, J. Cai, Y. Y. Xu, et al. 1997. The MAD-related protein Smad7 associates with the TGFβ receptor and functions as an antagonist of TGFβ signaling. *Cell.* 89:1165–1173.

54. He, W., D. C. Dorn, H. Erdjument-Bromage, P. Tempst, M. A. Moore, et al. 2006. Hematopoiesis controlled by distinct TIF1γ and Smad4 branches of the TGFβ pathway. *Cell.* 125:929–941.

55. Heldin, C. H., and A. Moustakas. 2006. A new twist in Smad signaling. *Dev. Cell.* 10:685–686.

56. Levy, L., and C. S. Hill. 2006. Alterations in components of the TGF-β superfamily signaling pathways in human cancer. *Cytokine Growth Factor Rev.* 17:41–58.

57. Chen, R. H., R. Ebner, and R. Derynck. 1993. Inactivation of the type II receptor reveals two receptor pathways for the diverse TGF-β activities. *Science.* 260:1335–1338.

58. Geiser, A. G., J. K. Burmester, R. Webbink, A. B. Roberts, and M. B. Sporn. 1992. Inhibition of growth by transforming growth factor-β following fusion of two nonresponsive human carcinoma cell lines. Implication of the type II receptor in growth inhibitory responses. *J. Biol. Chem.* 267:2588–2593.

59. Feng, X. H., E. H. Filvaroff, and R. Derynck. 1995. Transforming growth factor-β (TGF-β)-induced down-regulation of cyclin A expression requires a functional TGF-β receptor complex. Characterization of chimeric and truncated type I and type II receptors. *J. Biol. Chem.* 270:24237–24245.

60. ten Dijke, P., and C. S. Hill. 2004. New insights into TGF-β-Smad signalling. *Trends Biochem. Sci.* 29:265–273.

61. Ranganathan, P., A. Agrawal, R. Bhushan, A. K. Chavalmane, R. K. Kalathur, et al. 2007. Expression profiling of genes regulated by TGF-β: differential regulation in normal and tumour cells. *BMC Genomics.* 8:98.

62. Yang, W., R. R. Gomes, A. J. Brown, A. R. Burdett, M. Alicknavitch, et al. 2006. Chondrogenic differentiation on perlecan domain I, collagen II, and bone morphogenetic protein-2-based matrices. *Tissue Eng.* 12:2009–2024.

63. Gerdes, M. J., M. Larsen, L. McBride, T. D. Dang, B. Lu, et al. 1998. Localization of transforming growth factor-β1 and type II receptor in developing normal human prostate and carcinoma tissues. *J. Histochem. Cytochem.* 46:379–388.

64. O'Connor, J. C., M. C. Farach-Carson, C. J. Schneider, and D. D. Carson. 2007. Coculture with prostate cancer cells alters endoglin expression and attenuates transforming growth factor-β signaling in reactive bone marrow stromal cells. *Mol. Cancer Res.* 5:585–603.

65. Muntoni, S., S. Muntoni, and B. Draznin. 2008. Effects of chronic hyperinsulinemia in insulin-resistant patients. *Curr. Diab. Rep.* 8:233–238.

66. Segarini, P. R., D. M. Rosen, and S. M. Seyedin. 1989. Binding of transforming growth factor-β to cell surface proteins varies with cell type. *Mol. Endocrinol.* 3:261–272.

67. Goetschy, J. F., O. Letourneur, N. Cerletti, and M. A. Horisberger. 1996. The unglycosylated extracellular domain of type-II receptor for transforming growth factor-β. A novel assay for characterizing ligand affinity and specificity. *Eur. J. Biochem.* 241:355–362.

68. Peng, S. B., L. Yan, X. Xia, S. A. Watkins, H. B. Brooks, et al. 2005. Kinetic characterization of novel pyrazole TGF-β receptor I kinase inhibitors and their blockade of the epithelial-mesenchymal transition. *Biochemistry.* 44:2293–2304.